Chapter 4

Investigation of SiC/Oxide Interface Structures by Spectroscopic Ellipsometry

Sadafumi Yoshida, Yasuto Hijikata and Hiroyuki Yaguchi

Additional information is available at the end of the chapter

http://dx.doi.org/10.5772/61082

Abstract

We have investigated SiC/oxide interface structures by the use of spectroscopic ellipsometry. The depth profile of the optical constants of thermally grown oxide layers on SiC was obtained by observing the slope-shaped oxide layers, and the results suggest the existence of the interface layers, around 1 nm in thickness, having high refractive index than those of both SiC and SiO_2. The wavelength dispersions of optical constants of the interface layers were measured in the range of visible to deep UV spectral region, and we found the interface layers have similar dispersion to that of SiC, though the refractive indices are around 1 larger than SiC, which suggests the interface layers are neither transition layers nor roughness layers, but modified SiC, e.g., strained and/or modified composition. By the use of an in-situ ellipsometer, real-time observation of SiC oxidation was performed, and the growth rate enhancement was found in the thin thickness regime as in the case of Si oxidation, which cannot be explained by the Deal-Grove model proposed for Si oxidation. From the measurements of the oxidation temperature and oxygen partial pressure dependences of oxidation rate in the initial stage of oxidation, we have discussed the interface structures and their formation mechanisms within the framework of the interfacial Si-C emission model we proposed for SiC oxidation mechanism.

Keywords: SiC-MOSFET, SiC/oxide interface, spectroscopic ellipsometry, SiC oxidation mechanism, interface state density

1. Introduction

SiC metal-oxide-semiconductor field effect transistors (MOSFETs) are still the main targets in the research and development of SiC switching devices, because of their capability of ultra-low loss, high-frequency and high-temperature operation, and high-current and high-voltage tolerance, resulting in, for example, reducing the volume of electric power conversion modules compared with those using Si devices. However, SiC-MOSFETs have some problems to be solved before wide use, such as their higher on-resistance and lower reliability than those predicted from bulk properties. These poor device characteristics have been attributed to, for example, low carrier mobility due to high interface state density at the SiC/oxide interface and crystal defects. To elucidate the origin of poor characteristics of interfaces, it is important to make clear the interface structures as well as the study on the relation between interface structures and electrical properties.

1.1. Observation methods of interface structures

As metal-semiconductor and insulator-semiconductor junctions, and semiconductor hetero-junctions are key components of semiconductor devices, many measurement and observation techniques, e.g., X-ray photoelectron spectroscopy (XPS), transmission electron microscopy (TEM), scanning TEM (STEM), secondary electron microscopy (SEM), photoluminescence (PL) and cathodoluminescence (CL) spectroscopy, Rutherford backscattering spectroscopy (RBS), secondary ion mass spectroscopy (SIMS), have been adopted for the investigation of their interface structures. These techniques can be divided into three categories, i.e., (Figure 1)

1. observations of the interfaces on the cross section of specimens,
2. measurements of the thickness profile by etching or sputtering of the over or upper layers,
3. analysis of the signal coming from the interface through the upper layers.

In the cases of categories (1) and (2), there is a danger of the change and/or damage on the interface structures in the preparation process of specimens and by exposing the interface to the air, and a fear of non-uniformity of etching and/or sputtering of upper layers in an atomic layer thickness scale. In the case of cross-sectional TEM images, the specimen is required to reduce the thickness less than 100 nm. However, as the specimen is composed of still dozens of atomic layers, the image is formed by summing over the beams coming from a number of atomic layers in the specimen, and thus, it is hard to distinguish the effect due to the existence of interface layer from that of interface roughness and/or non-uniformity.

While, in the case of category (3), the observation is carried out without sample preparation, like thinning by etching and sputtering, and thus, there is no fear of the problems for the case of categories (1) and (2). In other words, the observation technologies belonging to category (3) are ideal ones which can observe the buried interface without any treatment, i.e., kept intact. However, this technique is only applicable to the case where the probing and signal beams from the interface can transmit through the upper or over layers, and thus, generally, the techniques are applicable only to the cases of very thin over layers or transparent ones for the

probe beam. Optical methods like ellipsometry and infrared reflectance spectroscopy, X-ray reflectivity (XRR), and RBS are the examples of the technologies of category (3). In the case of technologies of this category, however, as the signals from the interface are mixed with those from the upper and lower layers, it is necessary to analyze the signal under the assumption of a certain structural model. The information on interface structures is derived by the fitting of the calculated values by use of the model assumed and the observed data. Therefore, the results strongly depend on the model assumed, and thus, to build up an appropriate structural model is very important for obtaining significant information of interfaces from the observation. The model assumed is, in a word, a hypothesis, and thus, it is necessary to verify the validity of the model used. The influence of the selection of model used in the analysis of the obtained data will be discussed in the case of ellipsometric measurements of SiC/oxide interfaces in Section 2.

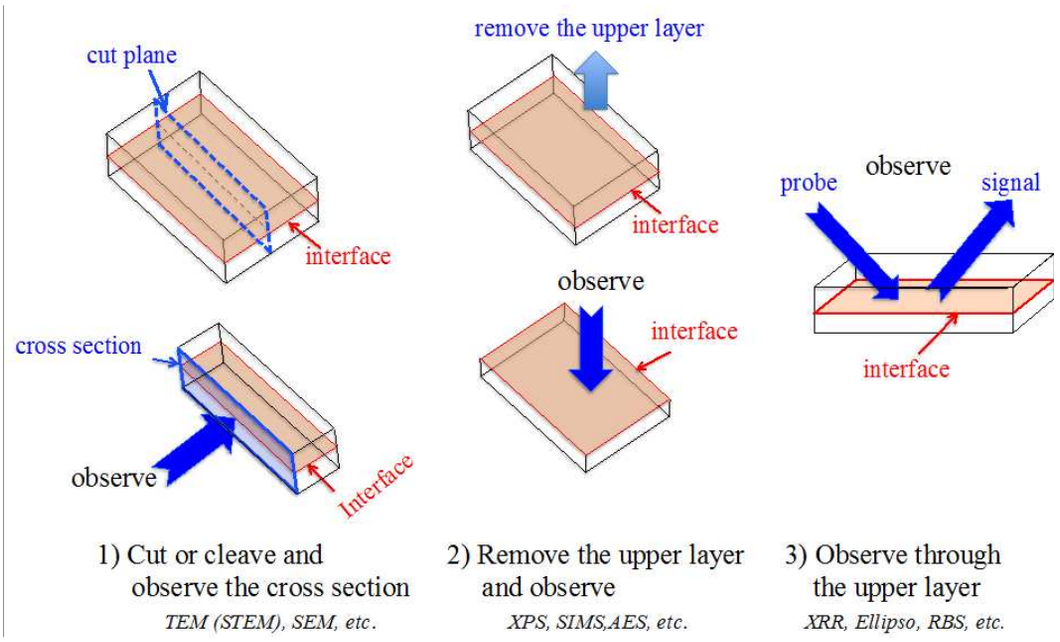

Figure 1. Three categories for the observation methods or techniques of interface structures.

1.2. Measurements by use of ellipsometry

As the oxide layers formed by thermal oxidation of SiC are transparent in the visible and ultraviolet spectral ranges, optical methods are suitable to detect the signal from the interface through the upper oxide layer. Especially, ellipsometry, i.e., the measurement of the changes in polarization upon the reflection of light from a surface, has very high sensitivity for very thin films because of the measurement of phase difference between p and s polarized light components and using oblique incident light beams, which brings about longer path in the films than those for perpendicularly incident light.

Many studies on the structures of Si/oxide interface by spectroscopic ellipsometry have been reported. Deal and Grove [1] measured the thickness of the thermal oxide on Si by using a

multiple beam interferometer in the range between 0.1 and 10 μm and derived the linear-parabolic model, so-called, D-G model, for Si oxidation. Taft and Cordes [2] reported the existence of the interface layers, 0.6 nm in thickness and 2.8 in refractive index by use of an ellipsometer at the wavelength λ = 546.1 nm. Aspnes and Theeten [3] have analyzed the interface structures in detail by spectroscopic ellipsometry. They proposed the equation to calculate the dielectric constants for two kinds of interface layers, i.e., physical mixture of amorphous Si and SiO_2, which corresponds to the cases of micro-roughness and inclusion or void in Si, and chemically mixed Si and O atoms. In the former, they used Bruggeman's effective medium approximation (EMA), and in the latter, they used Si-centered tetrahedral O atoms, $Si_{4-\nu}O$ (ν = 0-4) model by Philipp and composite medium theory by the Clausius-Mossotti relation. They reported that their results of spectroscopic ellipsometry for thermal oxides on Si are incompatible with either micro-roughness or an abrupt transition from Si to SiO_2, but rather support a graded transition layer, 0.7 ± 0.2 nm region in thickness of atomically mixed Si and O of average stoichiometry $SiO_{0.4\pm0.2}$. Massoud et al. [4] have performed in situ measurements of the thickness of Si oxides during the thermal oxidation in reduced oxygen partial pressure by the use of an automatic ellipsometer, and found the enhancement of the oxidation rate in thin thickness regime, which cannot be explained by the D-G mode, and showed good fit can be obtained by adding exponential term to D-G equation, though the physical meaning of adding new term, i.e., the origin of the exponential term, has not been ascertained. Nguyen et al. [5] found that the dielectric function of interface layers is similar to that of Si except the 0.02 eV red shift of inter-band critical point E_1 peak energy with rather small absolute values, from which they concluded there exist 2.2 nm thick interface layers composed of strained Si layer of 1.5 nm in thickness, and micro-roughness with 0.7 nm in optically equivalent thickness. They also said the transition layers reported by Aspnes and Theeten cannot be found, though the existence of the transition layers have been reported by using angle-resolved XPS, i.e., two monolayer compositional transition layers and one monolayer Si strained layer formed on a Si (001) face [6]. The refractive indices of very thin Si oxide layers were determined as a function of oxide thickness by ellipsometry using the thickness determined from tunnel current oscillation measurements [7]. Herzinger et al. measured the refractive indices of oxides on Si at the photon energy between 0.75 and 6.5eV by the use of variable-angle spectroscopic ellipsometry [8].

1.3. Observations of SiC/oxide interfaces

So far, many studies on SiC/oxide interface structures have been performed using various techniques, e.g., cross-sectional TEM and STEM belonging to category (1), and e.g., XPS and SIMS belonging to category (2). However, the results are sometimes contradicted with each other, and/or the results cannot be verified because of the fears mentioned above. For example, it has been reported that the SIMS measurement shows C atoms piled up near the interface more than 20%, and several percent even in Si oxide layers. On the contrary, it has been reported that XPS and medium energy ion scattering (MEIS) measurements suggest no such excess C around the interface and in the oxide films [9-11]. This contradiction is considered to be partly due to the difficulty in distinguishing between C atoms bonded to Si in adjacent SiC layers, the content of which is $10^{22}/cm^3$ order and excess C atoms near the interface in the case

of SIMS observation. In the case of XPS, C atoms bonded with Si and O can be distinguished between each other by the difference in their chemical shifts. As another example, Zheleva et al. [12] reported that high-resolution STEM combined with EELS measurements show the existence of interface layers, around 10 nm in thickness, with C-rich composition, and the thickness of the interface layers well correlates with the interface state density [13]. On the contrary, Hatakeyama et al. [14] reported that nosuch thick interface layer was observed by use of the same techniques, HAADF-STEM and EELS measurements, and, if there exists, it is less than 1 nm, which agrees with other measurements including our results by the use of spectroscopic ellipsometry.

Ellipsometry has been used mainly in the measurements of the thickness of oxide layers, where the interface structures were not taken into account. Suzuki et al. [15] and Zheng et al. [16] for 6H-SiC and Fung and Kopanski [17] for 3C-SiC measured oxide thickness by use of ellipsometry, and explained the oxidation time dependence of the oxide thickness by diverting the D-G model proposed for Si oxidation. Song et al. [18] measured oxide thickness of thermally grown oxide on 4H-SiC by use of RBS and spectroscopic ellipsometry, and found good agreement with each other, and they modified the D-G model in order to apply to SiC oxidation, i.e., adding the process of CO diffusing out from interface to surface as well as oxygen diffusion from surface to interface in the diffusion-limited regime, and used to explain their experimental results for oxidation time dependence of oxide thickness. It is noted that all of these measurements were performed by ex situ ellipsometry measurements, i.e., ellipsometric measurements were performed in air at room temperature after taking out from the oxidation furnace.

Sometimes, the thicknesses derived from the ellipsometry measurements are used as "physical thickness", or index of the progress of oxidation in the studies on, for examples, thickness dependences of some physical and chemical properties of oxide layers on SiC. If oxide layers are optically not uniform in the depth direction from SiC/oxide interface to oxide surface, and/or if the refractive indices of oxide layers are not same as those of stoichiometric SiO_2, e.g., there exist interface layers having different composition or properties from that of oxide layers, the thicknesses obtained are never physical thickness, because the thicknesses were derived under the assumption of an optically uniform single layer of stoichiometric SiO_2 on SiC with abrupt interface.

RBS, XRR, and Fourier-transformed infrared (FTIR) spectroscopy, the technologies belonging to category (3), have also been used to characterize SiC/oxide interfaces. RBS technique has been used mostly combined with ellipsometry. Ray et al. [19] measured oxide thickness by spectroscopic ellipsometry in the range thinner than 15 nm, and by RBS and ion channeling technologies as well as spectroscopic ellipsometry in the large thickness range, and studied on the oxygen partial pressure dependence of oxidation mechanisms and interface density by use of the analysis using the D-G model. Szilagyi et al. [20] measured oxide thickness and density by using spectroscopic ellipsometry and RBS, and roughness by atomic force microscopy (AFM), and the differences in oxidation process for Si- and C-faces of 4H-SiC were discussed comparing with that of Si. They also used modified D-G model to analyze oxidation mechanisms. A limited number of the results on the SiC/oxide interface structures obtained by use

of XRR and FTIR spectroscopy have been reported so far. The effects of NO annealing after oxidation of SiC to the interface structures and electrical properties were studied by use of XRR measurements for 6H-SiC [21] and 4H-SiC [22]. FT-IR spectroscopy by using attenuated total reflection (ATR) method has been performed to know the structures of the ultra-thin oxides on SiC [23,24]. The differences in stress and chemical state of oxides and oxide/SiC interface have been studied from the observation of TO and LO mode absorption due to Si-O-Si bond asymmetric stretching vibration for the oxides on Si- and C-faces of 6H-SiC and 4H-SiC.

We have employed spectroscopic ellipsometry for observing the SiC/oxide interface to investigate SiC/oxide interface structures. We have developed the characterization method of the oxide layers and SiC/oxide interfaces, i.e., the method using sloped oxide layers, and made clear the depth profile of the refractive indices and interface structures, i.e., there exist interface layers, around 1 nm in thickness, having high refractive indices [25,26], the values of which closely relate to the electrical properties of MOS diodes [27]. By the extension of measurement of wavelength to deep ultraviolet range, the structures of interface layers were discussed [28]. We have also developed the observation system in order to perform real time *in-situ* observation of SiC oxidation [29] for the first time. By using this system, we have found the enhancement of oxidation rate of SiC in thin-thickness regime less than several nm [30,31] as in the case of Si oxidation, and discussed on the oxidation and interface layer formation mechanisms [32]. These results have led to the proposal of a novel oxidation mechanism of SiC, i.e., "interfacial Si-C emission model" [33].

In this paper, the measurements of the depth profile of the refractive indices of thermal oxidation layers on SiC by using spectroscopic ellipsometry are described in Section 2, followed by the characterization of the interface layers, and their relation to the electrical properties of MOS diodes in Section 3, the real-time observation of SiC oxidation in Section 4, and the discussions on the SiC oxidation process and interface layer formation process based on SiC oxidation mechanisms in Section 5, and finally we summarize the investigations of SiC/oxide interface structures by using spectroscopic ellipsometry. All the spectroscopic ellipsometry measurements in this chapter were performed using a commercial spectroscopic ellipsometer typed GESP-5 (Sopra), typically at an angle of incidence of 75°.

2. Measurements of the depth profile of the refractive indices of thermal oxidation layers on SiC

2.1. Thickness dependence of apparent refractive indices of oxide films

The (0001) Si-faces of commercial 6H polytype SiC epilayers, 5 μm in thickness and n-type with the carrier concentration of 5×10^{15}cm^{-3}, were oxidized by two methods, pyrogenic oxidation and oxidation in dry oxygen flow, so-called dry oxidation [25]. Pyrogenic oxidation was conducted at 1100°C in a flow of oxygen and hydrogen gases for 1-8 h. Dry oxidation was conducted at 1000°C in a flow of oxygen for 4-16 h. Ellipsometry measurements were performed in the wavelength range from 250 to 850 nm. We have derived the optical constants

and the thickness of the oxide films under the assumption that the films have an optically single-layer structure and have uniform and isotropic optical properties. Here, we call the refractive indices obtained under the model of a single layer as "apparent refractive indices", in order to distinguish from those by use of a two-layers model mentioned in the next section. The wavelength dependence of the refractive indices of oxide films were assumed to follow Sellmeier's dispersion law,

$$n = \sqrt{1 + \frac{\left(n_{inf}^2 - 1\right)\lambda^2}{\lambda^2 - \lambda_0^2}}, \tag{1}$$

where parameter n_{inf} is the refractive index of the wavelength at infinity, while parameter λ_0 is the wavelength corresponding to characteristic oscillation. Here, we assumed the extinction coefficient $k = 0$ over the wavelength range measured. The values of the thickness of the film and the parameters n_{inf} and λ_0 were derived by fitting the wavelength-dependence curves of calculated ellipsometric parameters (Ψ, Δ) to the measured ones. The surface roughness of the oxide films on SiC was examined by means of atomic force microscopy (AFM) measurement, and the root mean square of the surface roughness is around 0.2 nm.

Figure 2(a) shows the wavelength dependences of the refractive indices of the oxide films, thickness of which are both 20 nm, oxidized with two different methods, i.e., pyrogenic and dry oxidation. For comparison, the values for oxide films on Si are also shown in the figure. It is found from the figure that the refractive indices of the oxide films on SiC are both smaller than those of the oxide films on Si at all the wavelengths measured. The figure also reveals that the refractive indices for dry oxidation are smaller than those for pyrogenic oxidation. The refractive indices increase with oxidation time or oxide thickness and reaching to the values for oxide films on Si, though the values of all the films are smaller than those of oxide on Si. The thickness dependences of the refractive indices at the wavelength of 630 nm for dry oxidation are shown in Figure 2(b). For pyrogenic oxidation, the refractive indices decrease with the decrease of film thickness as in the case of dry oxidation. It has been reported that, for Si, the refractive indices of the oxide films increase with the decrease of film thickness, as shown by the dotted line in the figures [7], which is quite different from those for the oxide films on SiC reported here. In Si oxidation, the increase of refractive indices along with the decrease of oxide thickness has been explained by the existence of the transition layers, i.e., suboxide layers SiO_x with $x < 2$ at Si/SiO_2 interfaces, whose refractive indices are larger than those of SiO_2, while the decrease of refractive indices for SiC oxidation cannot be explained by the existence of a $SiC\text{-}SiO_2$ transition layers. As the refractive indices of SiC are larger than those of SiO_2, the refractive indices of transition layer, i.e., the $SiC\text{-}SiO_2$ mixed layer SiC_xO_y should be larger than those of SiO_2.

As another candidate to explain these phenomena, the roughness of SiC/oxide interfaces can be considered. The roughness observed by AFM shows that there exists rugged structure with the various peak to valley height and interval over the surface much less than 1 nm, which are both much smaller than the wavelength of light used in ellipsometry measurements. In such a case, i.e., the case that the wavelength of a prove beam is much larger than the scale of surface

microstructures, the rough surface can be treated as the existence of an optically equivalent layer having the composition of the mixture of the adjacent layers of interface. Therefore, the refractive indices of optically equivalent layers corresponding to rough interface are also the values between the refractive indices of SiC and those of SiO_2, i.e., larger than those of SiO_2, and thus small refractive indices of oxide films cannot be explained by the effect of interface roughness.

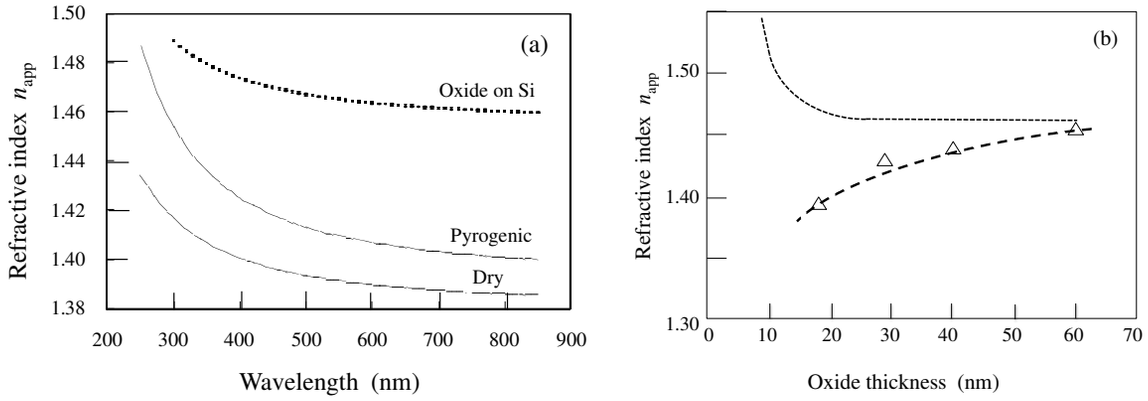

Figure 2. (a) Wavelength dependences of the refractive indices of oxide films formed by dry and pyrogenic oxidation. (b) Oxide thickness dependence of refractive indices of oxide films by dry oxidation. The dotted lines show the values for oxide film on Si [25].

2.2. Measurements of the depth profile of the refractive indices using sloped oxide films

In the previous section, the apparent refractive indices n_{app} obtained under the assumption of an optically single layer structure are shown to be smaller than those of the oxide films on Si, and increase with oxide film thickness, reaching the values of Si oxides of around 60 nm in thickness. To make clear why these apparent refractive indices change with oxidation time or oxide thickness, the depth profile of the refractive indices of oxide films on SiC was measured by spectroscopic ellipsometry [26].

For measurements of the depth profile or thickness dependence of the refractive indices of oxide films, we have proposed the method of using a slope-shaped oxide films. The pieces of SiC substrates with oxide layers were immersed gradually in buffered hydrogen fluoride at a constant speed to form slope-shaped oxide layers. The schematic illustration of the method is shown in Figure 3 [34]. Using the sloped oxide films, it is possible to measure the optical properties of the oxide films having various thicknesses using one sample. This means only the film thickness changes along the slope, though the interface structures are the same for all positions, i.e., for all oxide thicknesses. Of course, oxide films with various thicknesses can also be obtained by changing the oxidation time. By this method, however, there is a fear of change in the film structures, particularly the interface structures with the oxidation time.

(0001) Si-faces of n-type 6H-SiC epilayers having 5 μm in thickness and the carrier concentration of 5×10^{15} cm^{-3} were used for the study. The epilayer surfaces were oxidized in dry oxygen flow at 1100°C for 16 h to form the oxide films with around 60 nm in thickness. The sloped

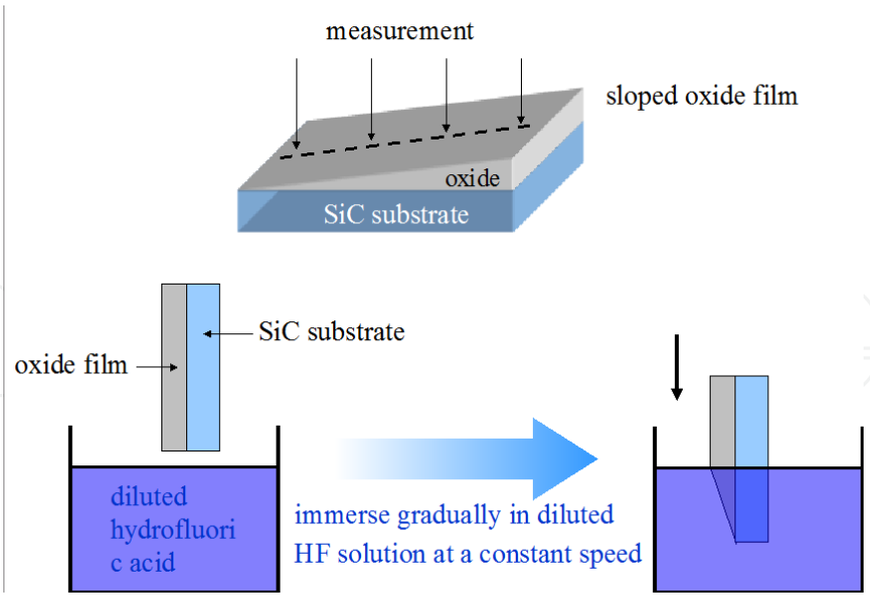

Figure 3. Schematic illustration of the method to fabricate a slope-shaped oxide film on SiC.

oxide films were fabricated by the method mentioned above, and ellipsometry measurements have been carried out at the positions along the slope.

Firstly, we have obtained the apparent refractive indices and film thickness assuming an optically single-layer structure with uniform optical properties, same as in Section 2.1. The variations of oxide thickness in the measured position along the slope are shown in Figure 4(a). From the figure, it is found that the oxide thickness changes almost linearly with the position, except in very small oxide thickness region, which means that the oxide films were etched at an angle as expected. Figure 4(b) shows the changes in n_{app} along the slope at the wavelength λ = 630 nm, for example. Figure 5 shows those as a function of oxide thickness. The refractive indices decrease with film thickness at all the wavelengths measured as in the case at 630 nm. It is found from the figure that n_{app} at 60 nm in thickness is around 1.45, which is almost the same as that reported for stoichiometric SiO_2, i.e., fused quartz. With the decrease of oxide film thickness, the value of n_{app} decreases gradually. At the positions with oxide thickness smaller than 5 nm, the values of n_{app} decrease markedly with the decrease of oxide thickness and approaches 1 at the position of the oxide film thickness = 0. As this feature is nearly the same as those observed for the oxide films formed by other oxidation methods mentioned in Section 2.1, it can be said that n_{app} decreases with decreasing oxide film thickness regardless of the oxidation method.

These results contradict the assumption used for the evaluation of the refractive indices and the thickness from the measured ellipsometeric parameters, i.e., the films are composed of optically single layers and have uniform and isotropic optical properties. This contradiction, therefore, suggests that this assumption is inadequate for the analysis. Then, we have considered the film structure models that can explain the thickness dependence of the refractive indices obtained from the ellipsometry measurements. For the oxide films on Si, it has been said there exists a compositional transition layer at the interface between Si and oxide [7]. Similarly, for the oxide films on SiC, it can be considered the presence of a transition layer at

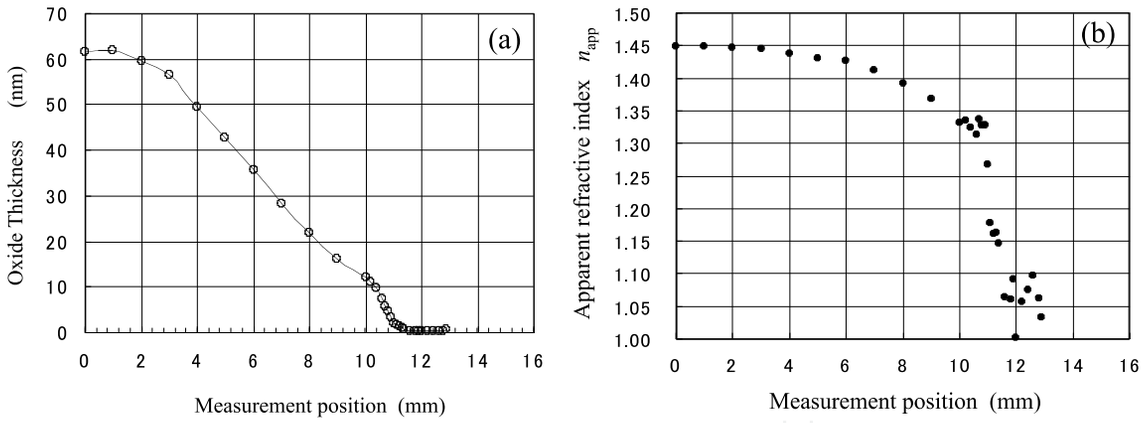

Figure 4. (a) Oxide thickness and (b) apparent refractive indices (λ = 630 nm) of a sloped oxide film on SiC along the slope [26].

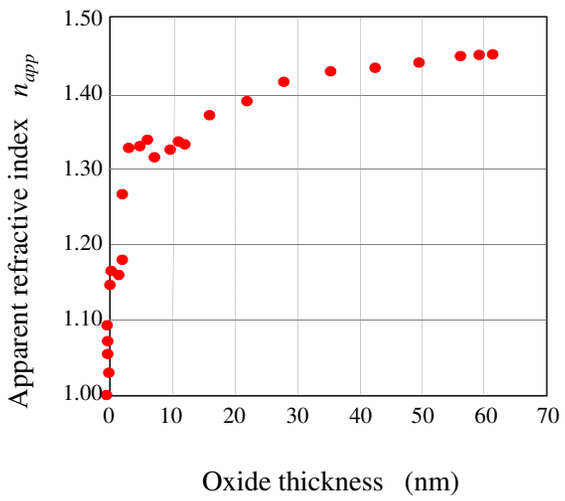

Figure 5. Thickness dependence of n_{app} of an oxide film on SiC at λ = 630 nm [26].

the interface between SiC and oxide layer. However, we have failed to explain the thickness dependences of n_{app} observed by the model taking into account the presence of the transition layer, the optical constants of which changes gradually from those of SiC to those of SiO_2.

Then, we attempted to obtain the optical properties of interface layers under the assumption of two-layers structure model, i.e., the structure of stoichiometric SiO_2 layer/interface layer/SiC substrates. Here, we assumed the presence of interface layers, not a transition layer but the layer having the wavelength dependence of the refractive indices of the interface layers that follows Sellmeier's dispersion law given by Eq. (1). We have used the optical constant of fused quartz for stoichiometric SiO_2. We have obtained the fitting parameters n_{inf} and λ_0 appeared in Eq. (1) and the thicknesses of interface layer and SiO_2 layer from the ellipsometry parameters measured as a function of wavelength. Figures 6(a) and (b) shows the values of the thicknesses of the SiO_2 layers and the interface layers, and the values of n_{inf} and λ_0, obtained at each measurement position, respectively. It is found from the figures that the thickness of

the SiO_2 layer changes almost linearly along the slope, and the thickness and the parameters n_{inf} and λ_0 of the interface layers do not change but are almost constant over the positions measured. These results indicate that the thickness dependence of n_{app} in oxide films on SiC can be explained by changing the thickness of the SiO_2 layer only, which suggest that the SiO_2 layer lies on the interface layer having the refractive indices given by the Sellmeier's equation with the parameter values n_{inf} ~4 and λ_0 ~ 0.15 and the thickness ~1 nm. As the parameter n_{inf} in Sellmeier's equation indicates the refractive index at long wavelengths, this means that there exist interface layers, around 1 nm in thickness with the refractive indices higher than those of SiC and SiO_2 (n = 2.6 and 1.45 at λ = 630 nm, respectively). These results strongly suggest that the interface layers are not mixed layers between SiC and SiO_2, i.e., neither transition layers nor optically equivalent layer due to interface roughness.

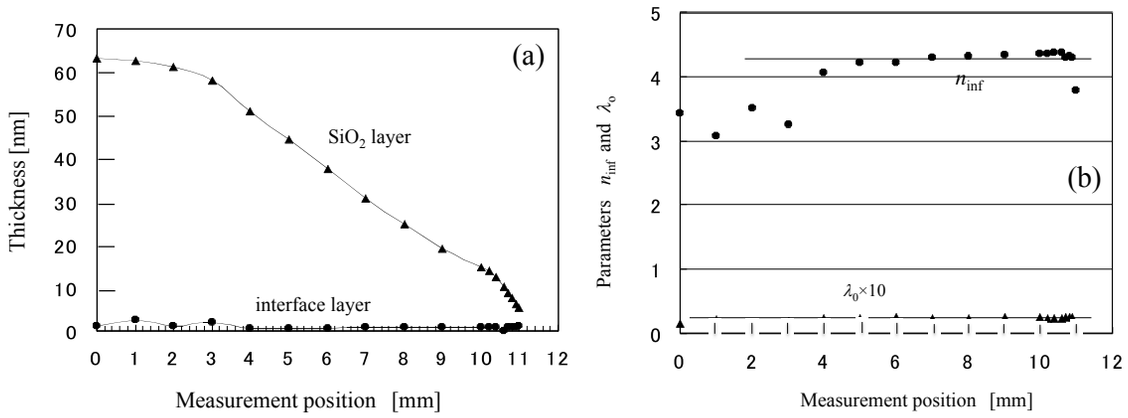

Figure 6. (a) Thicknesses of the SiO_2 and the interface layers, and (b) the Sellmeier's parameters n_{inf} and λ_0 of the interface layers as a function of the measurement position [26].

We have derived the refractive indices of the interface layers n_{it} as a function of wavelength on the assumption of the Sellmeier's dispersion law for refractive indices and the extinction coefficient k_{it} = 0. This is not self-explanatory in general. Then, we attempted to derive the optical constants of the interface layers at each wavelength from the measured (Ψ, Δ) values without using any assumption for optical constants [35]. The results reveal that the values of extinction coefficient are in the order of 0.1 though the values vary widely. The values of the refractive indices obtained at each wavelength almost agree with the values calculated from the values of n_{inf} and λ_0 obtained under the assumption of k_{it} = 0 and the Sellmeier's dispersion law for n_{it}. These results suggest that the assumption of the Sellmeier's dispersion law for n_{it} is also reasonable.

We have analyzed the interface layers for various formation methods of oxide, i.e., dry oxidation and low-temperature deposition of oxide (LTO), as well as pyrogenic oxidation. Dry oxidation was done in the pure oxygen flow at 1100°C for 16 h. Pyrogenic oxidation was done in a hydrogen-oxygen flame at 1100°C for 8 h. LTO films were deposited by low-pressure chemical vapor deposition (LPCVD) using SiH_4 and O_2 gases at 400°C and post-oxidation annealing (POA) in Ar atmosphere was performed at 1200°C for 1 h [36]. For all of the samples, the values of parameter n_{inf} and λ_0 are almost constant against oxide film thickness. Therefore,

the results of the ellipsometric measurements along the slope of the oxide films can be explained by two-layers mode mentioned above regardless of oxide formation methods. All the values of the refractive indices calculated using the values of n_{inf} and λ_0 obtained for three oxide films are higher than those of stoichiometric SiO_2 and bulk SiC. The values of n_{inf} depend on the oxidation process, and the values for LTO films are smaller than those for pyrogenic and dry oxidation, though the values of λ_0 are not different largely among these three layers.

From these results, we can conclude that there exist interface layers, having high refractive indices compared with those of SiC and SiO_2, the values of which depend on the oxide layer formation method, around 1 nm in thickness, at oxide/SiC interface and only the thickness of the SiO_2 layers changes with oxidation time or oxide thickness. It can be said that the optical properties estimated form the analysis using the single layer model mentioned in the previous section, i.e., the oxide films are assumed to be optically uniform single layer on SiC, are "apparent" features and it is not true that the optical constants of the oxide layers change with oxidation time or oxide thickness.

3. Characterization of the interfaces between SiC and oxides, and their relation to the electrical properties of MOS diodes

3.1. Characterization of the optical properties of interface layers between SiC and oxide

In the previous sections, it is said that the refractive indices of interface layers depend on the oxide layer formation process. For example, the values of n_{inf} for LTO films are smaller than those of pyrogenic and dry oxidation, while the LTO films are known to have lower interface state densities and effective oxide charge density than those of thermally oxidized films. Therefore, these results suggest the values of n_{inf} of the interface layers may be related to the electrical properties of SiC MOS structures in some extent. The large refractive indices evaluated suggest the existence of bonds with large polarization, like Si-Si bonds at the interface, which may influence on the electrical properties of the interfaces.

We have evaluated the oxide/SiC interfaces by spectroscopic ellipsometry measurements in the spectral range between 1.4 and 4.3 eV in Section 2. It has been reported in the studies on Si/oxide interfaces that the wavelength of optical constants in the absorption region, i.e., direct interband transition region, gives the information on a structural defect near the interfaces, such as oxide-induced stacking fault [37] and interface strain [5] because these defects bring about the shift of peaks corresponding to critical point. For Si, the absorption peak corresponding to E_1 (3.35eV) point locates in the visible to ultraviolet (UV) spectral range as shown in Figure 7 [38,39]. Therefore, the measurements in visible and ultraviolet spectral ranges can be reflected from the direct optical transition of Si. The band gap energy of 4H-SiC, for example, is 3.2 eV, which can be covered in the measurements mentioned above i.e., 250-850 nm or 4.96-1.46 eV. However, its absorption is very small up to around 4eV because SiC is an indirect energy bandgap semiconductor, and the absorption rises up near the direct transitions, for example, E_0 (5.65eV for 4H-SiC) [40]. Thus, the measurements including the deep UV (DUV)

spectral range may be capable to give more information on the SiC/oxide interface structures. Therefore, to obtain the information on the properties in direct interband transition region, we have expanded the wavelength range of the spectroscopic ellipsometry to deep UV region, i.e., to 200 nm, or 6.0 eV, which covers the E_0 peak of 4H-SiC [28].

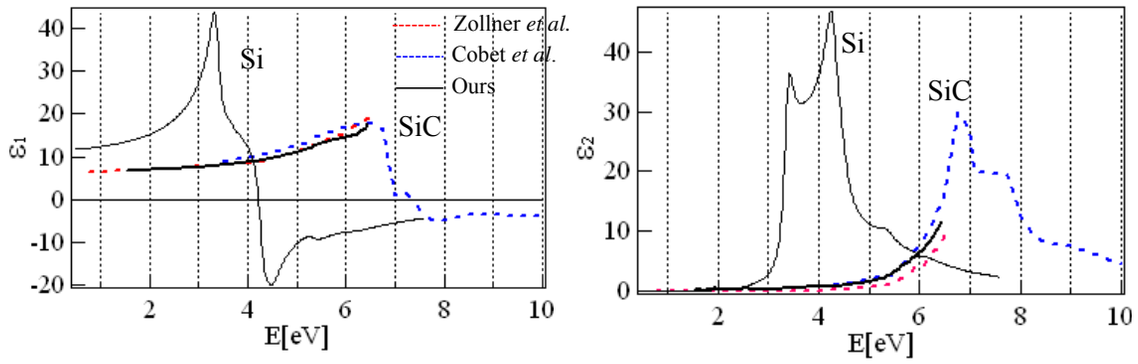

Figure 7. Photon energy dependences of the real and imaginary parts of dielectric constants for bulk Si and 4H-SiC [38,39].

Epitaxial wafers of 4H-SiC with 8° off-oriented (0001) Si-faces, n-types, were used in this study. A sample was oxidized at 1100°C in a dry oxygen atmosphere. By the oxidation for various time from 2.4 to 14.5 h, we obtained the oxide layers from 15.5 to 42.2 nm in thickness. The ellipsometric measurements were performed in the photon energy range between 2.0 and 6.0 eV. For the analysis of oxide layers on SiC, we used a two-layers structure model, i.e., the oxide layers are composed of a SiO_2 layer having the refractive indices for stoichiometric SiO_2 composition and an interface layer lain on SiC. Firstly, in the energy range between 2.0 and 4.0 eV, we evaluated the thicknesses of oxide layer and interface layer by fitting the calculated (Ψ, Δ) spectra to the measured values in this energy range. Here, we used the modified Sellmeier's dispersion relation, which takes into consideration of weak absorption, because the optical absorption of the interface is considered to be quite small in this photon energy range.

$$\varepsilon_1 = 1 + \frac{\left(n_{inf}^2 - 1\right)\lambda^2}{\lambda^2 - \lambda_0^2}, \quad \varepsilon_2 = \frac{C_1}{\lambda} + \frac{C_2}{\lambda^2} + \frac{C_3}{\lambda^3}, \tag{2}$$

where ε_1 and ε_2 are the real and imaginary parts of dielectric constant, respectively, n_{inf} and λ_0 are the refractive index of the wavelength at infinity, and the characteristic oscillation wavelength, respectively, and C_1, C_2, and C_3 are the fitting parameters for the optical absorption, so that we could obtain the thickness and optical constants of the interface layer as well as the SiO_2 layer thickness. After the determination of the SiO_2 and interface layer thicknesses in 2.0-4.0 eV range, by using these thickness values, the optical constants (n_{it}, k_{it}) of the interface layer were evaluated at each photon energy in the entire range from 2.0 to 6.0 eV from the ellipsometric parameters (Ψ, Δ) measured at the corresponding energies.

The thicknesses of the interface layers obtained are almost constant around 1 nm for all the oxide thicknesses measured. Figure 8 shows the photon energy dependence of n_{it}, and $k_{it,}$ of the interface layer at various oxide thicknesses from 15.7 to 42.2 nm. In the figure, the values of n and k for 4H-SiC are also shown by the red-colored lines. The values of optical constants in the range between 2 and 4 eV derived at each photon energy agree well with those obtained by use of the Sellmeier's relation determined by curve fitting in the same energy range. This agreement indicates that the structural model used in the analysis of ellipsometric data is appropriate. The figure suggests that the photon energy dispersion of n_{it} is quite similar to that of SiC, though the absolute values are around 1 larger than those of SiC, and slightly decreases with oxide thickness, and the differences between the interface layer and SiC tend to increase with photon energy. The photon energy dispersion of k_{it} is seen to be quite similar to that of SiC in entire energy range, i.e., nearly zero below 4 eV and a rise at around 5 eV.

The experimental results can be summarized as follow. There exists an interface layer of about 1 nm in thickness, though the absolute values of refractive index are 0.5-1 larger than that of SiC. The optical constants of the interface layer have similar energy dispersion to those of SiC in the photon energy range from 2.0 and 6.0 eV. These results indicate the existence of an interface layer, the material of which has a similar band structure as that of SiC. This leads the conclusion that the interface layer is not the transition layer between SiC and SiO_2, but a material having the modified structure and/or composition from SiC.

In the case of the thickest oxide sample, the energy where k_{it} rises up is smaller than that of bulk 4H-SiC. Nguyen et al. [5] evaluated the photon energy dependence of the dielectric constants of the interface layers for Si and found a red shift of 0.042 eV of the interband critical point E_1 (3.35eV) compared with the bulk silicon values, and concluded there exists a strain layer of Si by the compressive stress due to the lattice expansion by oxidation, as well as the layer due to rough interface or transition of composition less than 0.7 nm in thickness. Our result of the increase of k_{it} in the deep UV region for the thickest oxide of SiC can be explained by the red shift of E_0 peak of SiC due to the increase of interfacial strain accompanied with oxidation, because the expansion of Si bond due to oxidation is expected also for SiC.

We will discuss on the formation mechanisms and the structures of interface layers in Sections 4 and 5, relating with the oxidation mechanisms of SiC.

3.2. Relation between the optical and electrical properties of interface layers

i. Performance of spectroscopic ellipsometry measurements and *C-V* measurements on the same samples

It is found that there exist interface layers around 1 nm in thickness and the refractive indices n_{it} depend on the oxidation conditions, i.e., oxidation method and oxidation temperature, which suggests that the values of n_{it} may reflect the change of the interface structures to some extent. Under these considerations, we have tried to investigate SiO_2/4H-SiC interfaces by using capacitance-voltage (*C-V*) measurements and FTIR spectroscopy, in parallel with spectroscopic ellipsometry measurements [41]. In the cases of the oxide layers formed by dry oxygen, we found high densities of interface trap, larger shift of *C-V* curve along the gate

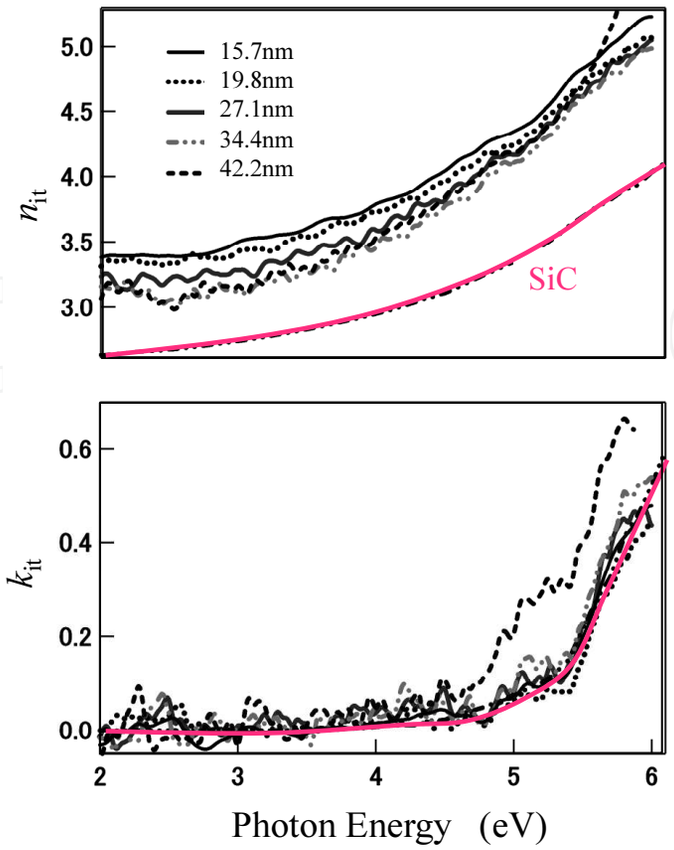

Figure 8. The photon energy dependences of optical constants, n_{it} and k_{it}, of the interface layers at various oxide thicknesses for oxide films on Si-face of 4H-SiC by dry oxidation [28].

voltage axis and large leakage current from *C-V* measurements. FT-IR measurements suggest lower vibration frequency of the Si-O-Si stretching mode compared to that of fused quartz.

Based on these preliminary results, we have performed systematic studies on the SiC-oxide interfaces fabricated by various oxidation methods grown on SiC (0001) Si- and (000-1) C-face surfaces to make clear the relation between the refractive indices of interface layers derived from spectroscopic ellipsometry measurements and the interface sate densities derived from *C-V* measurements [27]. *C-V* measurements were performed on the same samples used in the ellipsometric measurements for the purpose of direct comparison between optical and electrical characteristics. Based on the results obtained, we have discussed on the structures of SiC/oxide interfaces related to the interface states which degrade the electrical properties of SiC-MOS structure, like channel mobility of the carriers.

For optical measurements, we have evaluated the refractive indices of the interfaces n_{it} from the ellipsometric measurements by the analytical methods mentioned in the previous section as well as the results from XPS measurements [42]. To keep high sensitivity in the measurements over the wide photon energy range, i.e., wide spectral range from deep UV to visible range, the measurements were carried out at the different angles of incidence of 70° and 75° for 1.5-2.0eV and 2.0-6.4 eV, respectively. For electrical measurements, we have performed

high-frequency *C-V* measurements at 1 MHz for the same samples used in the optical measurements to evaluate interface state density D_{it} by way of the Terman method.

These optical and electrical measurements using same samples have been carried out for the oxides grown on SiC with various growth conditions, i.e., dry and wet oxidation at 1000°C and 1100°C for Si-face, and dry oxidation at 900, 1000, and 1100°C, and wet oxidation at 900, 950, and 1000°C for C-face, as well as the samples with post-oxidation annealing. By using the results obtained from the measurements, we have compared the growth condition dependences of optical and electrical properties, i.e., refractive indices of interface n_{it} and interface trap density D_{it} to make clear the correlation between n_{it} and D_{it}.

ii. Dependences of n_{it} and D_{it} on oxidation temperature, oxide method, and surface polarity

Figures 9 and 10 show the values of optical constants n_{it} and k_{it} as a function of photon energy, and D_{it} as a function of energy from the Fermi levels, for Si-face and C-face, respectively, oxidized by wet and dry oxidation at various oxidation temperatures. It is found from Figure 9 that the values of n_{it} and D_{it} for wet oxidation are both larger than those for dry oxidation, and both change little with oxidation temperature for Si face. While for C-face, as seen in Figure. 10, the values of n_{it} and D_{it} for dry oxidation are both larger than those for wet oxidation, and both change remarkably with oxidation temperature and increase with increasing oxidation temperatures for dry oxidation. Contrary, for wet oxidation, D_{it} increases with increasing temperature as in the case of dry oxidation, but n_{it} increases, i.e., the oxidation temperature dependences of n_{it} has opposite tendency for dry oxidation. These results are summarized in Tables 1(a) and (b) for temperature, surface polarity and oxidation method dependences. We have found that the growth condition dependences of n_{it} are well corresponding to those of D_{it}, though the case of C-face oxidized by wet oxidation is an exception. The reasons of this exception have been discussed elsewhere [27], comparing with the researches on the oxidation temperature and oxidation method dependences of D_{it} reported [36, 43-45].

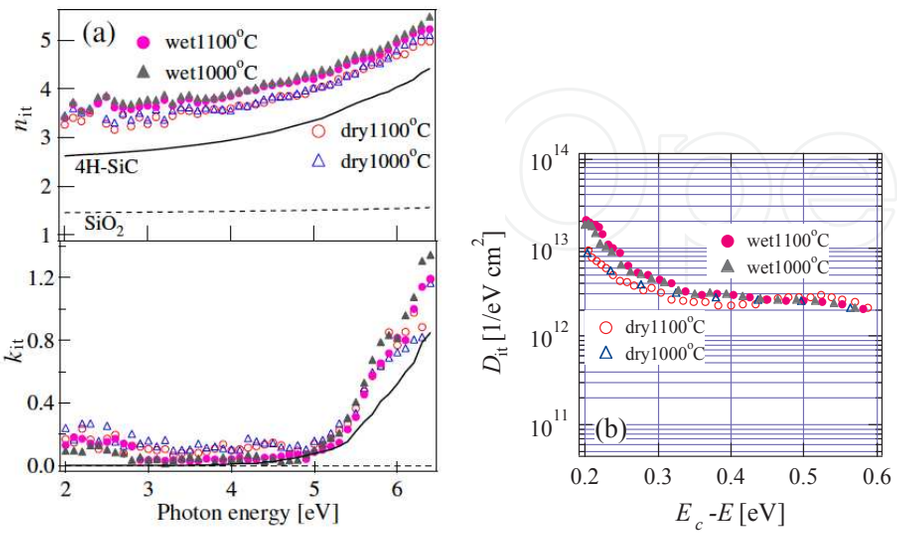

Figure 9. Refractive index, n_{it}, and extinction coefficient. k_{it}, of the interface layer (a), and interface states density D_{it} (b), for Si-face. The solid and broken lines in (a) show the optical constants of SiC and SiO_2, respectively [27].

The differences in D_{it} for oxidation method, surface polarity and oxidation temperature have been reported by many researchers and the origins have been studied by use of, for example, XPS [46] and EPR [47].

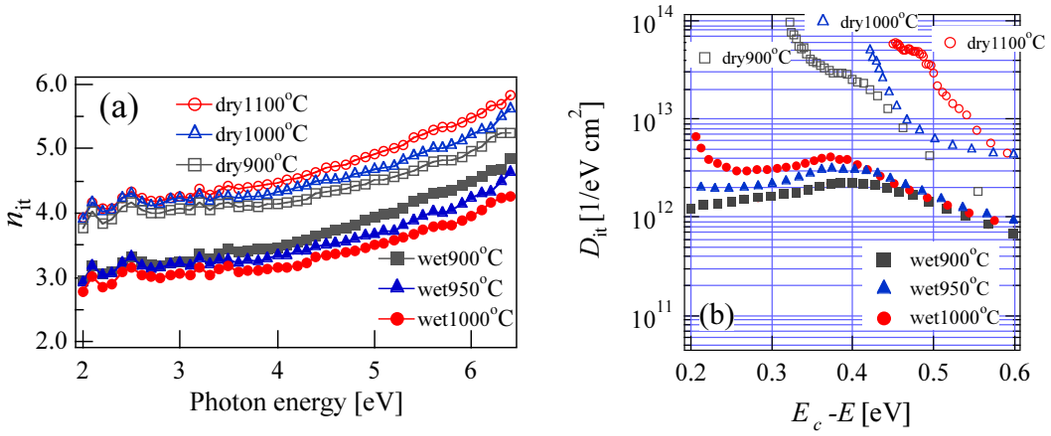

Figure 10. Refractive indices of the interface layer n_{it} (a), and interface states density D_{it} (b), for C-face [27].

(a) Temperature dependences

polarity	Si-face	C-face
dry oxidation	small change	small change
wet oxidation	increase	decrease

(b) Oxidation method and polarity dependences

Si-face・dry	<	C-face・dry
∧		∨
Si-face・wet	>	C-face・wet

Table 1. Oxidation temperature (a) and oxidation method and polarity dependences (b) of both the refractive indices of interface n_{it} and interface state density D_{it}

iii. Effect of post-oxidation annealing on n_{it} and D_{it} for wet oxidation

To understand the differences in n_{it} and D_{it} by oxidation method, we have performed post-oxidation annealing (POA) in Ar and O_2 atmosphere at 600°C for 3 h for wet oxidation samples based on the results reported [25]. Figures 11 and 12 show n_{it} and D_{it} values for Si- and C-face, respectively, with and without POA. The figures reveal that, for both polarities, the values of n_{it} and D_{it} come close to those for dry oxidation by POA. From these, it is considered that as grown samples by wet oxidation, hydrogen-related species terminate the dangling bonds of Si or C at the interface, and then they are removed by POA, which brings about the interface characteristic close to those for dry oxidation. The changes by annealing in oxygen and argon atmosphere are almost the same with each other for Si-face. Contrary, for C-face, the changes by annealing in oxygen are much larger than that in argon atmosphere, which is considered to be due to the oxidation even at around 600°C for C-face.

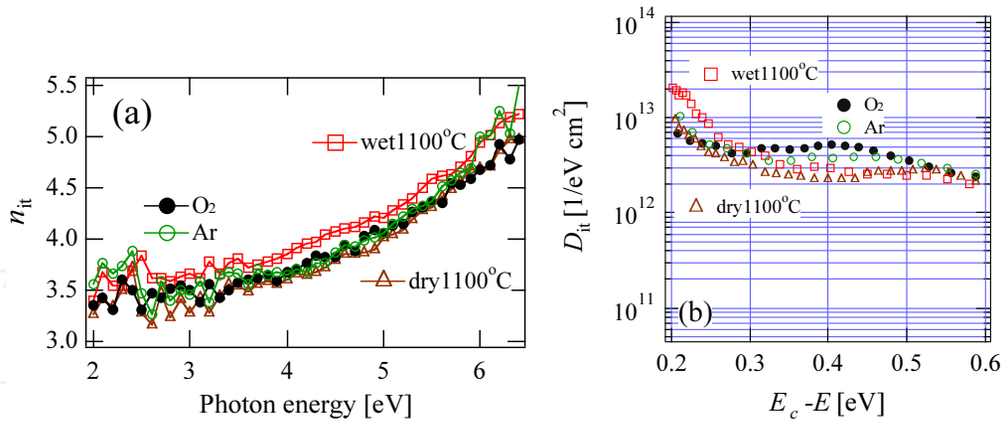

Figure 11. Changes in n_{it} (a) and D_{it} (b) on Si-face by POA for wet oxidation [27].

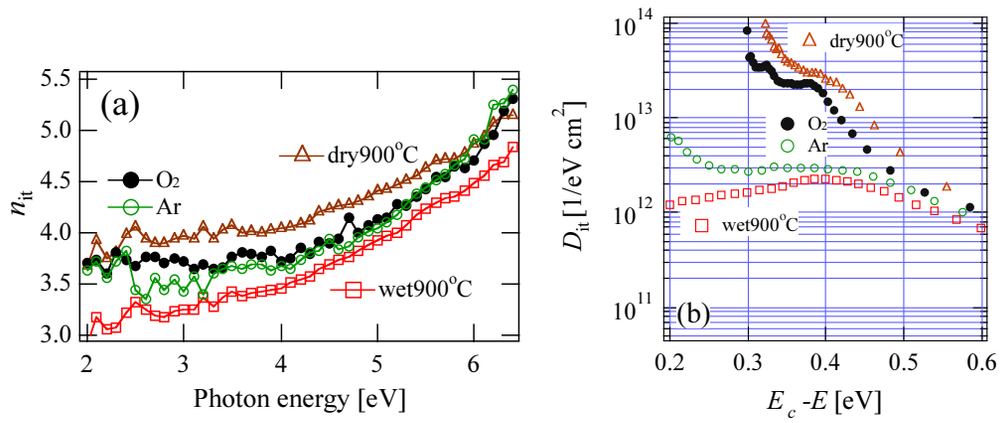

Figure 12. Changes in n_{it} (a) and D_{it} (b) on C-face by POA for wet oxidation [27].

iv. Effect of the change in oxidation rate on n_{it} and D_{it} for C-face

In Figures 9 and 10, the measurements were performed on the samples oxidized at the same temperatures for Si- and C-faces to know the surface polarity dependences of n_{it} and D_{it}. It is well known that the oxidation for C-face is around 10 times faster than that for Si-face. Therefore, these results were obtained from the oxides with different oxidation rates for C- and Si-faces. Then, we have prepared oxide films grown with same growth rate to avoid the influence from the growth rate to polarity dependence. The oxidation rate for C-face at 850°C is reported to be almost same as that for Si-face at 1100°C. The values of n_{it} and D_{it} for dry oxidation of C-face at various oxidation temperatures between 800°C and 1100°C as well as those of Si-face at 1100°C are shown in Figure 13. It is found from the figure that the differences in n_{it} and D_{it} between the oxides for C-face at low temperatures and those for Si-face grown at 1100°C considerably reduce with decreasing oxidation temperature, which suggests that the lowering in the oxidation rate is quite effective for reducing n_{it} and D_{it} values. However, the method of changing oxidation temperature is possible to result in the change of the oxidation reaction process. Therefore, we have prepared the samples for C-face oxidized at the same temperature, 900°C, but with low oxygen partial pressure between 0.4 and 0.6 atm. However,

similar tendency in the case of decreasing oxidation temperature for the values of n_{it} and D_{it} were obtained [27].

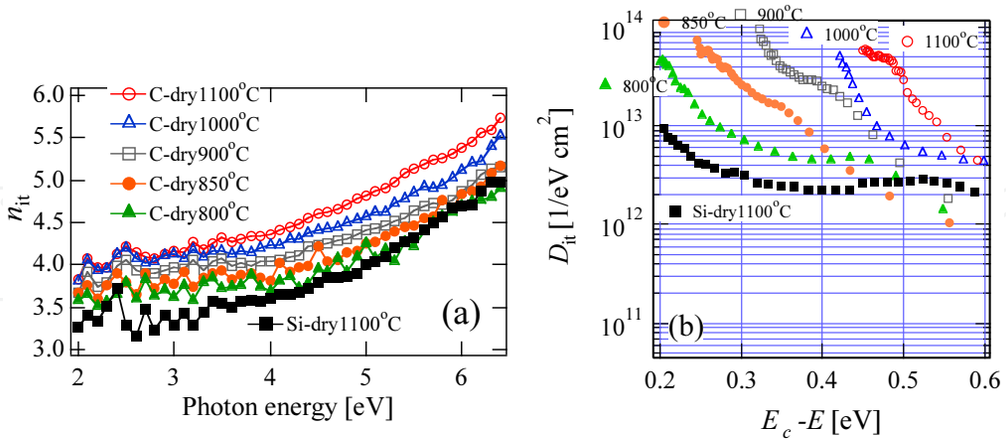

Figure 13. The values of n_{it} (a) and D_{it} (b) on C-face at oxidation temperatures between 800°C and 1100ºC [27].

v. Verification of the correlation between n_{it} and D_{it} of interface layers by γ-ray irradiation

We have found the refractive indices of interface layers measured by spectroscopic ellipsometry correlate well with the interface state density estimated by *C-V* measurements. To verify this correlation quantitatively, it is necessary to perform quantitative comparison between the changes of the interface state density and the refractive indices of the interfaces. It is well known that γ-lay irradiation brings about the increase of interface state density. Therefore, the quantitative correlation between the change in the refractive indices and interface state densities can be studied by performing *C-V* and ellipsometric measurements using the samples increased in interface state density artificially by γ-ray irradiation.

We have prepared the samples, interface state density of which were increased by γ-ray irradiation, and, for these samples, we have performed *C-V* and ellipsometric measurements before and after γ-ray irradiation [48]. Si-face of 6H-SiC with epilayers, 5 μm in thickness and n-type, 5 × 10^{15}cm^{-3} were used. The epilayers were oxidized at 1100°C for 2 h by pyrogenic oxidation method to form oxide layers, around 30 nm in thickness. The ellipsometric measurements were carried out for the slope-shaped oxide films formed by gradually immersing the samples into BHF solution at a constant speed. After the optical measurement, the oxide layers were removed. Then, the samples were oxidized again, and Au and Al electrodes for gate and ohmic contacts, respectively, were formed on oxide layer and back surface of SiC substrate to form MOS diodes.

After *C-V* measurements, the samples were subjected to ^{60}Co γ-ray for various duration times from 1 to 38 h (0.4-14.7 kC/kg with the rate of 2.58-3.87×10^2C/kg h) at room temperature, and again *C-V* measurements were carried out. Finally, after the electrodes were removed, slope-shaped oxide films were formed and ellipsometric measurements were carried out. Optical analysis is the same as in the cases of that mentioned in the previous sections, i.e., using two-layers model composed of a SiO_2 layer and an interface layer on SiC. The values of n_{inf} and λ_0

parameters appeared in the Sellmeier's dispersion equation Eq. (1) for the interfaces of samples before and after γ-ray irradiation were measured.

The results reveal the values of n_{int} increases, while that of λ_0 show little change by γ-ray irradiation, i.e., the refractive indices of interface layer increase by γ-ray irradiation. The changes in the value of n_{inf}, Δn_{inf} and interface state density, ΔN_{it}, are plotted as a function of absorption dose, where N_{it} (cm^{-2}) is the integration of D_{it} ($eV^{-1}cm^{-2}$) by energy, and are shown in Figure 14 (a). Figure 14 (b) shows the relation between Δn_{inf} and ΔN_{it}. The figure shows there exists a strong correlation between them, almost linear relation, though the data points are not so much. This result suggests the values of refractive indices of interface obtained from ellipsometery measurements are well reflected from the electrical properties of interface, like interface state density. Finally, it should be noted about the influence of γ-ray irradiation to the SiO_2 layers. We have confirmed that the influence on the derivation of the refractive indices of the interface layers by the change in refractive index of SiO_2 layer by γ-ray irradiation, around 0.02, is small enough to neglect.

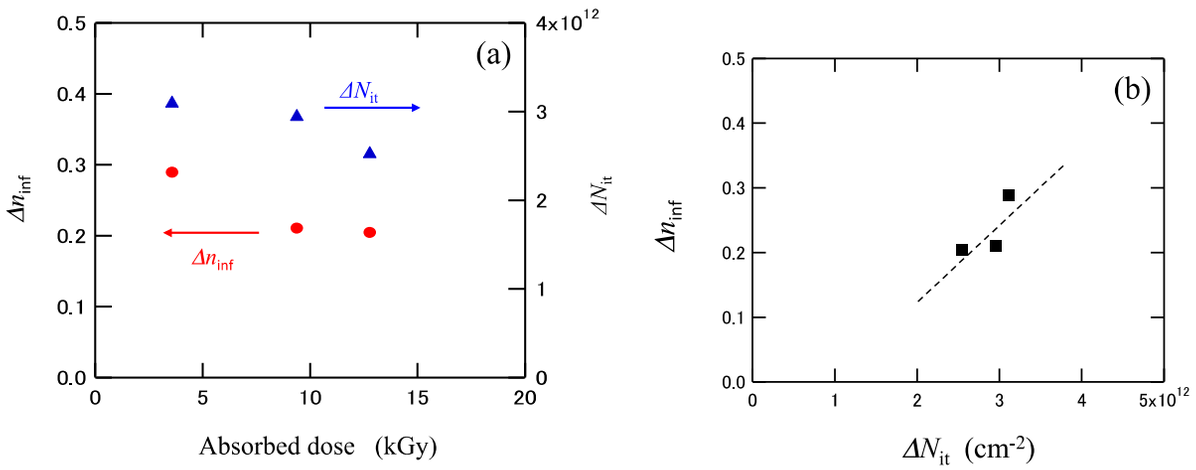

Figure 14. (a) Changes in n_{inf}, Δn_{inf} and interface state density, ΔN_{it}, as a function of γ-ray absorption dose, and (b) the relation between Δn_{inf} and ΔN_{it}.

4. Real-time observation of SiC oxidation

4.1. Real-time observation of SiC oxidation using an in situ spectroscopic ellipsometer

We have found that, in the thermal oxides on SiC, there exist interface layers, around 1 nm in thickness, with the optical constants having similar energy dispersion with SiC, though absolute values of refractive indices are around 1 higher than that of SiC. And, we also found that the values of refractive indices correlate well to the interface state density. As the interface structures may form during the oxidation, the interface structures should be closely related to oxidation mechanisms of SiC, and therefore, it is necessary to study the oxidation mechanisms to know the formation mechanism of the interface layer i.e., to make clear the origin of interface layers observed, which may lead how to reduce the interface state density at the SiC-oxide interface. Therefore, in order to elucidate the origin of the interface states, it is also important

to know the mechanism of SiC oxidation, especially at the initial stage of oxidation. For these requirements, the precise measurements of oxidation rate, especially in very thin-thickness regime, are indispensable. Many studies have been performed on the oxidation time dependences of oxide films of SiC by use of various methods, including spectroscopic ellipsometry for various SiC polytypes [15-18,20]. In these studies, however, the measurements were performed after the oxidation, i.e., *ex-situ* measurements, where accurate oxide thickness as a function of oxidation time cannot be obtained because the oxidation proceeds even during rising and dropping in substrate temperature. Especially in small thickness range, i.e., the initial oxidation stage, this inaccuracy may bring about the difficulty in the precise study on the oxidation process. Therefore, to study on the mechanism of SiC oxidation in more detail, especially in initial stage of oxidation, a real-time observation technique is indispensable.

We have developed an in situ ellipsometric measurement system, composed of a lamp-heated furnace and a spectroscopic ellipsometer (SOPRA,GESP5), to observe the SiC oxidation in real time. The details of the system are described elsewhere [29]. Figure 15 (a) illustrates schematically the in situ spectroscopic ellipsometer we designed. The furnace has two optical windows for incident beam and reflected light beam from the sample surface for ellipsometric measurements. The fused quartz glass windows are angled so that the surfaces of the window glass are normal to the incident and reflected beams, i.e., inclined ±15° from the normal direction of the sample surface, to perform the ellipsometric measurements at an angle of incidence of 75°. The samples were heated up to a prescribed temperature between 600°C and 1200°C by the IR beam from a halogen lamp focused on the sample surface through the guiding quartz rod. The temperature of the samples was measured by using an IR radiation thermometer. The furnace was evacuated by a turbo molecular pump down to 2×10^{-6} Pa and Ar gas was introduced into the chamber during the measurement of optical constants of SiC substrate before oxidation at the oxidation temperature. Oxidations were performed by introducing dry oxygen and wet oxygen for dry and wet oxidations, respectively.

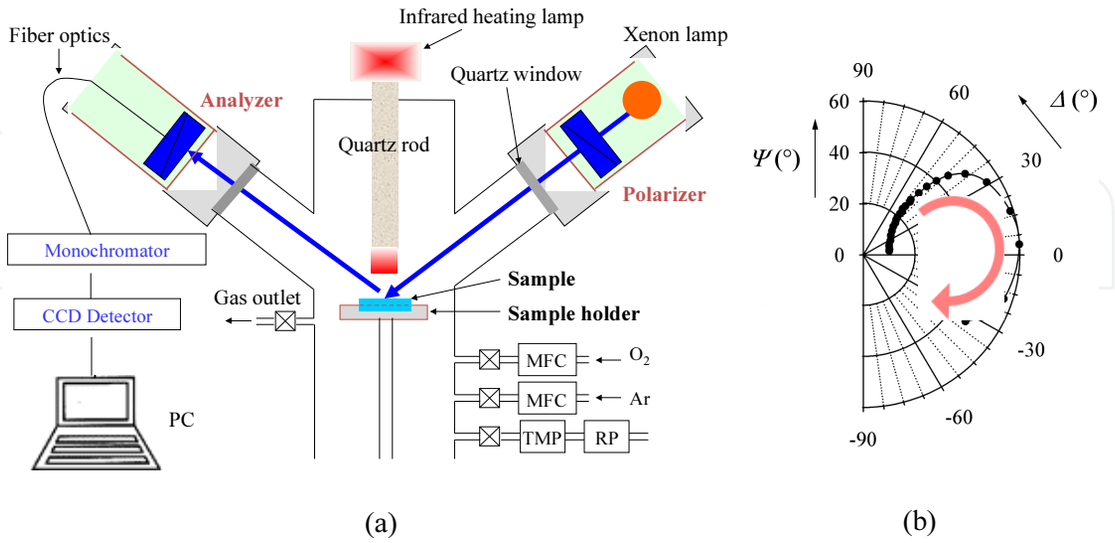

Figure 15. (a) Schematic diagram of the in situ spectroscopic ellipsometer we designed, and (b) an example of the observed values of (Ψ, Δ) over the oxidation time range from 5 min to 6 h in the case of the oxidation temperature 972°C. The values of Ψ and Δ are plotted in the radius and angle in this pole figure, respectively.

Figure 15 (b) shows an example of the observed values of (Ψ, Δ), plotted on a pole figure coordinate, over the oxidation time range from 5 min to 6 h at 972°C. The experimental points (Ψ, Δ) move clockwise with oxidation time. It should be noted the merit of pole figure, i.e., Ψ and Δ are shown by the radius and angle, respectively. Comparing with a right angle coordinate, there is no jump but connected at 0° and 360° or 2π in Δ, and the figure reveals that the precision of Δ depends on the absolute values of Ψ.

We have carried out real-time *in-situ* measurements at various growth temperatures between 893°C and 1147°C. The oxide thicknesses are plotted as a function of oxidation time in Figure 16. Compared with the previously reported results obtained from *ex situ* measurements [15,18], it is found from the figure that the data during the initial oxidation stage were obtained with much improved detail and much smaller spread.

For Si thermal oxidation, Deal and Grove [1] have considered two rate-determining processes, i.e., the reaction process at the interface and the process of oxygen diffusion through the oxide layer, and proposed, so-called, D-G-model, given as,

$$X^2 + AX = B(1+\tau) \tag{3}$$

where, X, t and τ are the oxide thickness, oxidation time, and initial oxidation time, respectively. B/A and B are denoted as the linear and parabolic rate constants of oxidation, respectively. Many researchers have applied D-G model to explain SiC oxidation [15, 18]. We also applied the D-G model to the results obtained from in situ ellipsometric measurements. The fitted curves derived using Eq. (3) are shown by the broken lines in Figure 16, which reveals that the fits are good at all the oxidation temperatures in our experiments. However, there is a discrepancy between the values of B/A and B obtained in this study and those reported by, for example, Song et al. [18], who modified D-G model for Si oxidation to that for SiC by taking into account the presence of carbon, i.e., adding the out diffusion process of CO from the interface to the surface. One of the reasons of this discrepancy is considered to be the difference of measurement method, i.e., the *ex-situ* measurements performed after the oxidation have been used in the previously reported studies, while we used *in-situ* real-time measurements and thus, the relations between oxide thickness and oxidation time can be precisely obtained. The reasons of these discrepancies in the values of rate constants appeared in D-G model between ours and those by Song et al. have been discussed in details by Goto et al. [49] with the relation of the oxide growth rate enhancement in thin thickness regime for SiC oxidation.

4.2. Oxide growth rate enhancement of SiC in thin oxide regime

In the previous section, we mentioned that real-time observation of SiC thermal oxidation using an *in-situ* ellipsometer has been performed for the first time and shown that the results are well explained by the D-G model. However, it has been reported that the oxidation behavior of Si in thin oxide thickness range cannot be explained using the D-G model, where the oxide growth rate enhancement has been found. Therefore, we have studied the initial oxidation stage of SiC in more details to make clear such an oxide growth rate enhancement occurs also for SiC or not.

http://dx.doi.org/10.5772/61082

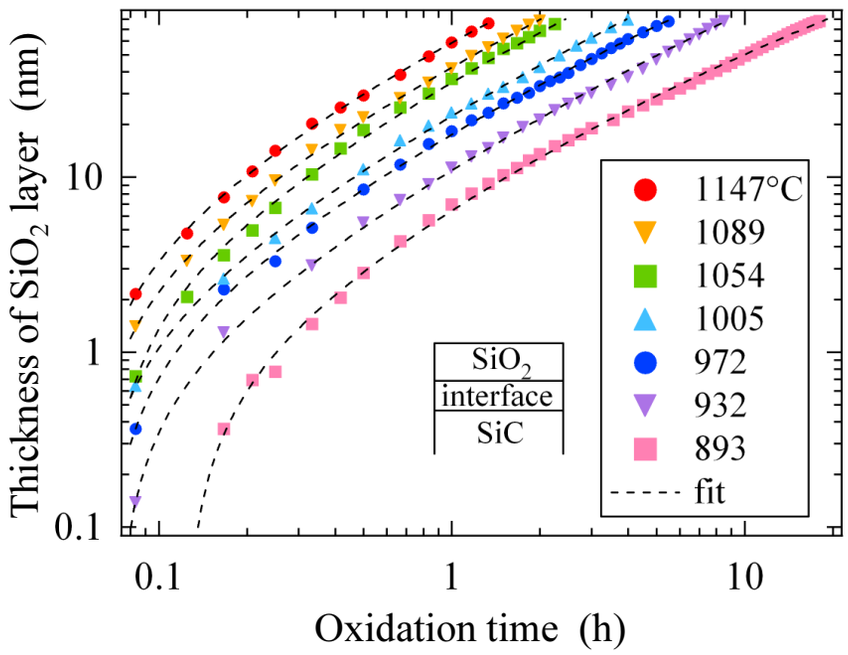

Figure 16. Oxide thickness as a function of oxidation time at various oxidation temperatures. The broken lines show the fitting curves by use of D-G model [29].

In the study mentioned in Section 4.1, the real-time measurements of (Ψ, Δ) were performed at the single wavelength $\lambda = 400$ nm. In order to observe the oxidation in initial oxidation stage, i.e., to elucidate the oxidation process and interface layer formation in more detail, we have undertaken the spectroscopic observation of SiC oxidation by using a CCD detector. We have performed the measurements of oxidation rate in thin-thickness regime both for C- and Si-faces of 4H-SiC by in situ real-time observation using a spectroscopic ellipsometer with CCD detector [30,31,50].

Ellipsometric measurements were carried out at wavelengths between 310 and 410 nm, where we can perform the ellipsometric measurements without the disturbance by the strong light emission from the heated sample. We have derived the thickness of oxide layers as a function of oxidation time by using the same analytical method mentioned in the previous sections.

Firstly, we have applied the D-G model to the results obtained at various oxidation temperatures. Though the fits are seen in general well over the wide thickness range in the thickness range of thinner than around 20 nm, it was found there exists a tendency for the observed values to be slightly larger than the calculated ones by using the D-G model. To see these discrepancies in more detail, we have derived the oxidation rates dX/dt from the observed curves of oxide thickness X(t).

Figure 17 shows the oxide thickness dependences of oxidation rate for C-face and Si-face. The figures reveal that the values of the oxidation rate including the thin thickness range of less than 10 nm can be obtained by real-time in situ spectroscopic observation. However, the figures also suggest that the oxidation rates calculated using the D-G model cannot be fitted to the

observed ones over the entire oxide thickness range at all the oxidation temperatures measured, though the fitting is well in the range thicker than around 20 nm for C-face and several nm for Si-face, as shown by the solid lines in Figure 17(a). While, in the thin thickness region, the oxidation rates are larger than the values calculated by use of the D-G model regardless of oxidation temperature. These results reveal that the oxidation having a larger growth rate than that predicted by the D-G model occurs in thin-thickness range, though the critical thickness is different between C-face and Si-face.

By the D-G model, the relation between the growth rate dX/dt and the oxide thickness X is given [1] as,

$$\frac{dX}{dt} = \frac{B}{A + 2X}. \tag{4}$$

In small thickness range, i.e., $X \ll A$, the oxidation is limited by the reaction rate at the interface, and the growth rates are constant, equal to B/A from Eq.(4). However, the experimental results shown in Figure 17(b) reveal that, the growth rates are not constant but increase with decreasing oxide thickness in small thickness range. These experimental results for C- and Si-face suggest that the oxidation enhancement occurs regardless of surface polarity.

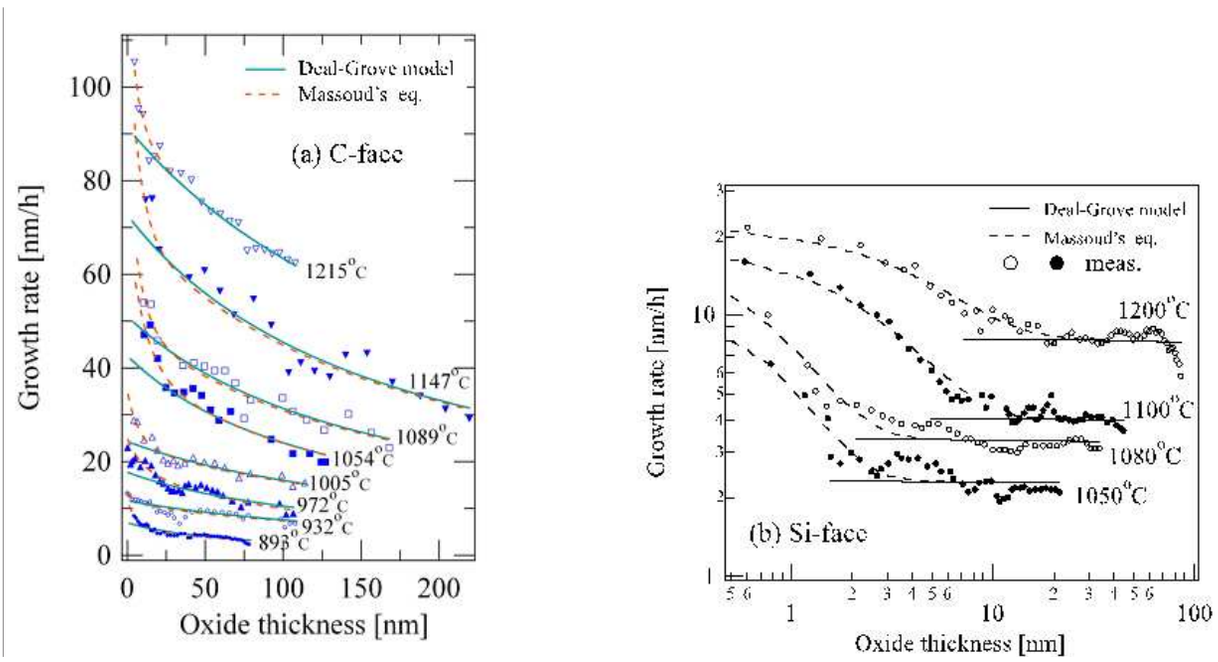

Figure 17. Oxide thickness dependences of oxide growth rates at various oxidation temperatures for (a) C-face, and (b) Si face [30,31].

4.3. Application of Massoud's empirical equation to SiC oxidation

Many researchers have tried to explain the oxide growth rate enhancement in thin-thickness regime for Si oxidation [4,51-54]. Massoud et al. [4] have proposed an empirical equation giving

the oxidation rate as a function of oxidation thickness by adding an exponential term to the D-G equation, as,

$$\frac{dX}{dt} = \frac{B}{A+2X} + C\exp\left(-\frac{X}{L}\right), \tag{5}$$

where C and L are the pre-exponential constant and the characteristic length, respectively.

We have tried to fit the calculated values to the observed ones by use of Eq. (5) for both Si- and C-faces. In all the oxidation temperatures, much better fittings than those using Eq. (4) were obtained, as shown by the broken and solid lines, respectively, in Figures 18 (a) and (b). From the curve fitting, the values of L as well as C, B/A and B were derived. Both for Si- and C-faces, the values of L scarcely depend on the oxidation temperature, around 7 nm, the behavior of which is almost the same as that for the oxidation of Si [4]. These results suggest that oxidation enhancement is predominant when oxide thickness is smaller than around 7 nm for both faces of SiC and Si oxidations.

i. Temperature dependences of oxidation rates

We discuss the temperature dependences of the four parameters B/A, B, C, and L below. Figure 18(a) shows the Arrhenius plots of the linear rate constant B/A for C-face and Si-face. The B/A values for C-face are one order of magnitude larger than those for Si-face at all the temperatures measured, which corresponds well to the experimental results that the growth rate of C-face is about 10 times larger than that of Si-face. The figure suggests that the values of B/A for Si-face lie on a single straight line having the activation energy of 1.31 eV, while for C-face the values lie on two straight lines the breaking point of which is around 1000°C. The activation energies for the higher and the lower temperature ranges are 0.75 and 1.76 eV, respectively. In this experiment, the growth rates of SiC for oxide thickness smaller than around 100 nm were measured. Therefore, we do not discuss the temperature dependences of the values of B here because of insufficient precision in determining the parabolic rate constant B without data for more thick oxide.

The values of $C/(B/A)$ are around 2-6 for Si-face, but for C-face smaller than 1. As the values of $C/(A/B)$ give the magnitude of oxide growth enhancement, the growth rate enhancement phenomenon is suggested to be more marked for Si-face than for C-face. The Arrhenius plots of the parameters C and L are shown in Figure 18(b). The figure reveals that the values of C for Si-face are almost independent of temperature, but those for C-face increase with the increase of temperature. While for the values of L, that for C face reveals little dependence on temperature, but that for Si-face steeply increase with temperature. The absolute values of L for Si face and C-face are around 3 and 6 nm, respectively, at 1100°C. It is found from the figure that the temperature dependences of C and L are different between Si-face and C-face of SiC. For Si oxidation, in comparison, it has been reported that L are around 7 nm and almost independent of temperature, and the values of C increase with temperature [4], which are the same for SiC C-face, but different for SiC Si-face. From these results, it can be said that the

oxidation mechanism of SiC C-face is similar to that of Si in some sense, while that of SiC Si-face is quite different from that of Si.

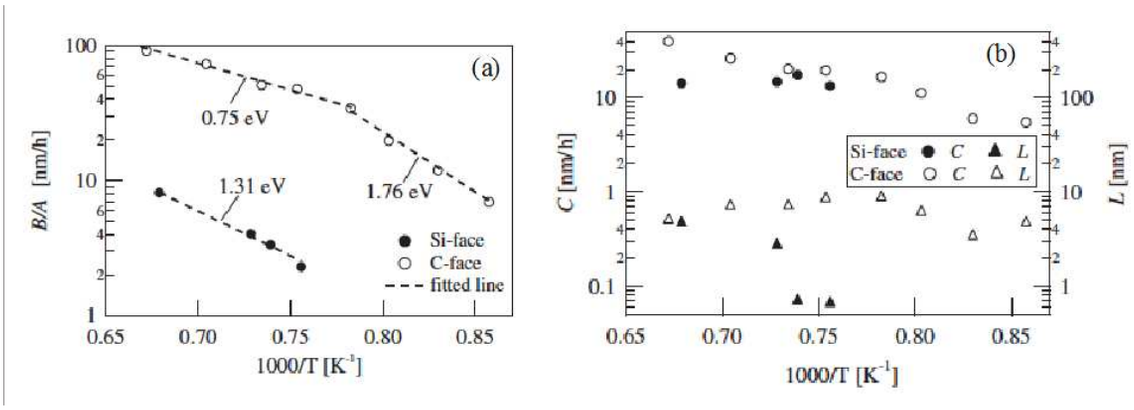

Figure 18. Arrhenius plots of the linear rate constant *B*/*A* (a), and *C* and *L* (b), for C- and Si-faces [31].

ii. Oxygen-partial-pressure dependence of oxidation rates

In the previous section, we have studied the temperature dependences of oxidation rate. Another parameter to control the oxidation rates is the quantity of oxygen supplied to the interface. Therefore, we have studied the pressure dependence of oxidation rate. Especially at reduced pressure, the oxidation rates become small, which is good to observe the initial oxidation stage in details.

Figures 19(a) and (b) show the oxide thickness dependence of oxide growth rate at various oxygen partial pressures for C- and Si-face, respectively. These figures reveal that the oxide growth rate enhancement occurs at any partial pressure, as in the cases at 1 atm. Figures 20(a) and (b) show the oxygen-partial-pressure, *p*, dependence of the values of the linear rate constant *B*/*A* and the enhancement parameters *C* and *L* for C-face and Si-face. It is found from Figure 20(a) that the values of *B*/*A* behave similar pressure dependences for both surface polarities, as ~ $p^{0.6}$. The D-G model [1] leads the results that *B*/*A* and *B* are proportional to *p*, which contradicts to our results, as well as for Si oxidation, i.e., ~ $p^{0.7\text{-}0.8}$ [4]. We have already reported that the value of *B* for both Si- and C-faces is proportional to *p* [50], which also contradicts to the prediction from D-G model. Figure 20(b) shows the variations of the values of *C* and *L* with oxygen pressure for Si- and C-faces. It is found from the figure that those values for both surface polarities are almost constant with respect to pressure, which is different from the pressure dependence of the values of *B*/*A* and B. The fact that the enhancement parameters *C* and *L* are independent of pressure, which is quite different from those for *B*/*A* and *B* values, suggests the existence of an additional oxidation-rate-limiting mechanism, which is independent of the quantity of oxygen supplied, other than the interface reaction of oxygen with SiC (*A*/*B*) and the diffusion of oxygen and CO through SiO_2 layers (*B*).

http://dx.doi.org/10.5772/61082

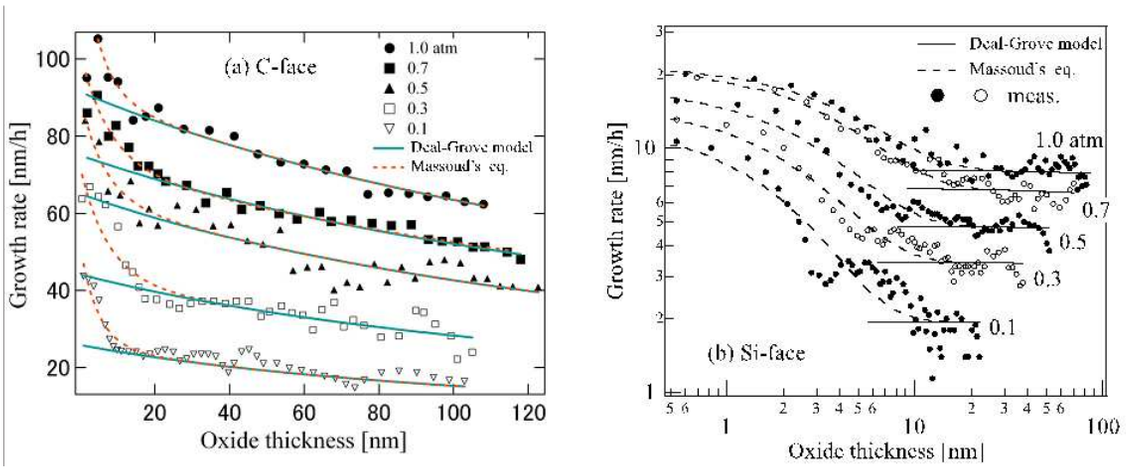

Figure 19. Oxide thickness dependences of oxide growth rates at various oxygen pressures for (a) C-face, and (b) Si-face [31,50].

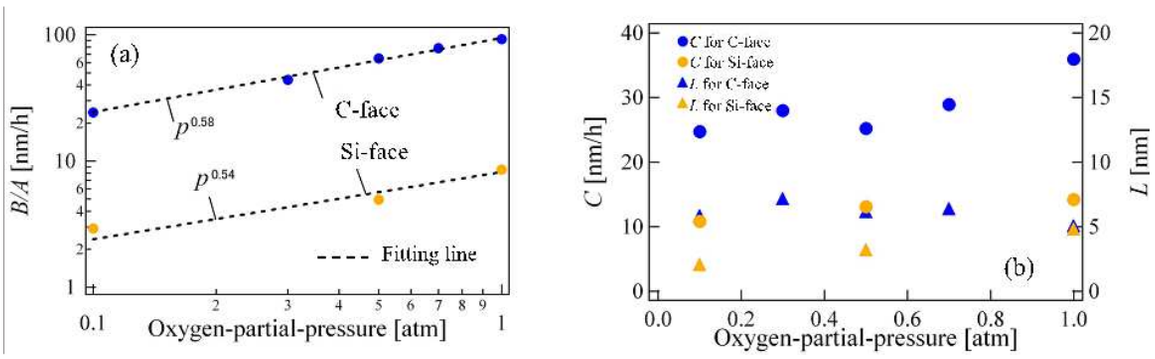

Figure 20. Oxygen pressure dependences of the values of the parameters, *B*/*A*, *C*, and *L* for C- and Si-faces [31].

5. Studies on the SiC oxidation process and interface formation based on SiC oxidation mechanisms

In the previous sections, we have studied SiC oxidation process by use of in situ real-time observation using automatic spectroscopic ellipsometry and found the oxidation rate enhancement in very thin-thickness regime, for the first time, which cannot be explained by using the D-G model. Then, we have applied Massord's equation proposed for the growth rate enhancement for Si, and discussed the oxidation temperature and oxygen partial pressure dependences of the parameters appeared in the equation. However, the Massord's equation was derived without considering any physical and/or chemical mechanisms of Si oxidation, i.e., the equation was derived for fitting to the experimental results on the oxide thickness dependence of growth rate. Therefore, the Massourd's equation (Eq.(5)) is one of the empirical equations, and thus, it may not be appropriate to discuss the physical or/and chemical meaning from the results of the nature of parameters in the equation.

Growth rate enhancement has been observed also for Si oxidation in thin-thickness regime. Kageshima et al. [52] and Uematsu et al. [55] have proposed the model for Si oxidation, called "interfacial Si emission model", where Si atoms are emitted into the oxide layers as well as into Si substrate, owing to the strain that arises from the expansion of Si lattices to form SiO_2 lattice. By the interfacial Si emission model, the oxidation rate at the interface is primarily large and becomes suppressed by the accumulation of emitted Si atoms near the interface with the progress of oxidation. This means that the oxidation rate never enhances in small thickness range but rapidly decreases with the increase of oxide thickness.

The interfacial Si emission model suggests that the stress near/at the oxide-Si interface originated from the formation of SiO_2 lattice brings about the growth enhancement in the initial oxidation stage. The density of Si atoms in SiC (4.80×10^{22} cm^{-3}) [56] is almost equal to that in Si (5×10^{22} cm^{-3})[57], which may bring about almost identical situation for SiC oxidation as in the case of Si oxidation. Therefore, it can be considered that the interfacial emission of atoms caused by the interfacial stress also brings about the growth enhancement in SiC oxidation. Based on these considerations, we have proposed the model, called "interfacial Si-C emission model", taking into account the presence of carbon in SiC to explain the experimental results for SiC oxidation reported [33],

As the formation of interface structures is considered to be closely related with the initial oxidation process, we have studied initial oxidation of SiC in more detail at reduced oxygen partial pressers, and discussed on the formation process of the interface layers in terms of SiC oxidation mechanism in ultra-thin-thickness regime. Though the oxide growth rate of SiC is much smaller than that of Si, it is still too fast to observe the initial growth process in detail. Therefore, a reduction in the growth rate, for examples, by lowering oxidation temperature, and/or lowering the oxygen partial pressure, is believed to be useful for observation of the initial oxide growth process of SiC more minutely. To make clear the oxygen partial pressure dependence of the SiC oxidation process, ex situ measurements have been carried out at the pressures from 10^{-3} to 4 atm [16,19]. However, the initial oxidation process has not been examined in detail, partly due to the limit of the precision of the data obtained by ex situ measurements in small thickness regime.

5.1. Observation of SiC oxidation in ultra-thin oxide regime at low temperatures

We have studied SiC oxidation at low temperatures or under reduced oxygen pressure in detail by performing in situ and real-time spectroscopic ellipsometry in ultra-thin oxide thickness regime [58]. Figures 21(a) and (b) show the oxidation time dependences of the thicknesses of SiO_2 and interface layer for the oxidation at 850° and 700°C, respectively, in the oxygen pressure of 1 atm. At 850°C, both the interface layer and the SiO_2 layer thicknesses increase with time, but the thickness of interface layer is saturated at about 1 nm by the oxidation time more than 2 h though the continuous increase in SiO_2 layer thickness is seen even after 2 h. While the oxidation at 700°C brings about the rapid increase of SiO_2 thickness up to around 1 nm and then the very small oxidation rate, resulting in the 1.2 nm in thickness even after 8 h oxidation. The figure also shows that the thicknesses of the interface layer are almost zero up to 8 h, indicating that no interface layer is formed between SiO_2 and SiC at 700°C. These results

suggest that an interfacial layer is not formed by low temperature oxidation, but is formed at 850°C. From the experimental results mentioned above, it is also possible to derive the conclusion that the interface layer is not formed or is extremely thin when the SiO_2 layer is thinner than around 1nm but is formed when SiO_2 thickness is over 1-2 nm. That is to say, there are two possibilities in the condition of realizing oxide layers on SiC with no interface layer, i.e., low oxidation temperatures or/and oxide layers thinner than around 2 nm. However, it is hard to study interface structure in this oxide thickness range at 850°C, because the oxide layer, around 1 nm in thickness, is formed in too short time to measure in details even at 850°C.

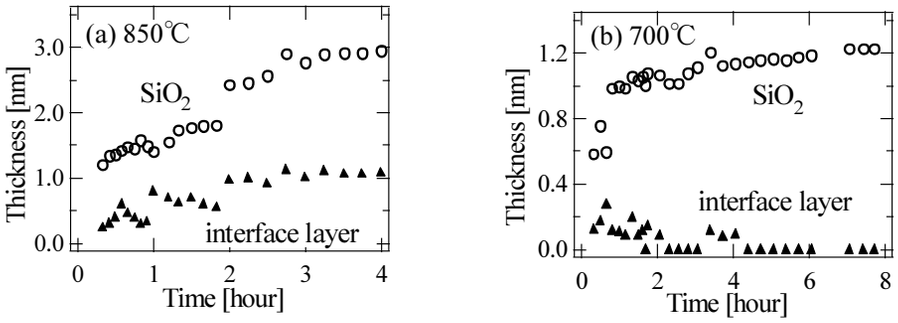

Figure 21. Oxidation time dependences of thicknesses of the SiO_2 layer and the interface layer for the oxidation at (a) 850°C and (b) 700°C [58].

By way of reducing the partial pressure during the oxidation, we have examined the oxidation at 850°C more precisely in order to clarify the formation process of interface layers. The reduction of oxygen pressure down to 0.01 atm brings about the oxidation rate almost the same as that of 700°C, 1 atm. At the reduced oxide growth rates, we can obtain the information about the interface layer in the thin oxide thickness range less than 1 nm even for the oxidation at 850°C. The results reveal that the interface layer thickness is extremely thin, when the SiO_2 layer thickness is smaller than ~1 nm. Therefore, the formation of an interface layer is considered to be independent of oxidation temperature but depends on the SiO_2 layer thickness. These results, as well as those in the study mentioned in Section 3.1, suggest that the interface layers are never transition layers between SiC and SiO_2, like as SiO_x, and/or SiO_xC_y, but the layers modified a little from SiC.

According to the interfacial Si-C emission model [33], Si atoms are considered to be emitted not only to oxide layer side but also to SiC substrate side. The Si atoms emitted into SiC may form SiC layers including Si interstitials near the SiC/oxide interface. The SiC layers with Si interstitial may have large refractive indices than SiC due to the large atomic density, but may have similar band structures due to, not the displacement of lattice sites, but the occupation of interstitial sites. Together with the experimental results that the interface layers have large refractive indices but have extinction coefficient just like SiC, the interface layers formed by SiC oxidation are supposed to SiC layers with interstitial Si atoms emitted from the interface accompanied by the oxidation of SiC. For Si oxidation, Nguyen et al. have found the existence of strained Si layers just near the Si/oxide interface and have attributed to the strain due to the expansion of Si lattices by oxidation [5]. As the red shift of th*e* E_0 gap energy is arose by the

tensile stress in Si, the layers having different optical constants from Si are formed near the interfaces. Similarly, for SiC, the stress due to the oxidation is considered to generate the layers having different optical constants from that of SiC near the interface. The stress is reported to cause the polytype conversion from 4H-SiC to 3C-type, which is also possible to change the properties of SiC near the interface. Based on the interfacial Si-C emission model, the fact that the interface layer is not formed or the thickness of the interface layer is very small for thin oxide layers can be understood as follows. As a strain at the interface is considered to increase with the increase of oxide layer thickness, the strain in thin oxide layers is very small, and thus a little amount of Si atoms are emitted, which results in no or very thin interface layer formed. The critical thickness of the oxides at which an interface layer forms, or the noticeable changes of optical constants occur in the SiC layer near the interface, may be around 1nm.

5.2. Observation of SiC oxidation in thin oxide regime and the discussion on SiC oxidation and interface formation mechanisms

In the previous section, we have studied the initial oxidation stage, up to several nm in oxide thickness, by use of oxidation at low temperatures or under reduced oxygen pressure up to several nm in thickness of oxide, and discussed the structure and formation mechanisms of interface layer. However, it is feared that the oxidation mechanism changes with oxidation temperatures, like lower than 1000°C. Therefore, we have studied the initial oxidation stage, up to several 10 nm in thickness, at reduced oxygen pressure down to 0.02 atm at 1100°C to discuss on the formation process of the interface layers in the frame of SiC oxidation mechanism, i.e., the interfacial Si-C emission model [33], in thin-thickness regime.

Epitaxial wafers of 4H -SiC with a 0.5° off-oriented (000-1) C-face and a 8° off-oriented (0001) Si-face, both are n-types, having a net donor concentration N_d - N_a = 3 × 10^{15} cm^{-3} and 1 × $10^{16}cm^{-3}$, respectively, were used in this study. All the oxidations were conducted at the oxidation temperature of 1100°C under various oxygen partial pressures between 0.02 and 1 atm. The obtained (Ψ, Δ) spectra were analyzed using a two-layers structure model and optical constants of the interface layers were assumed to follow the modified Sellmeier's dispersion relation taking a weak optical absorption into account, Eq. (2).

Figures 22(a) and (b) show the oxide thickness dependence of the interface layer thickness and those of n_{inf} of the interface layers on the SiC (000-1) C-face and (0001) Si-face, respectively. The values of n_{inf} for 4H-SiC and SiO_2 are also shown by the broken lines in the figures. As seen in Figure 22, the interface layer thickness increases with increasing oxide thickness and saturates around 1.5 nm at the oxide thickness of around 7 nm, and this saturation thickness depends slightly on the partial pressure. The figures also show that the values of n_{inf} are also saturated around 7 nm in oxide thickness and the saturated values depend slightly on the partial pressure.

The oxide thickness dependence of the oxide growth rates on the 4H-SiC C-face and Si-face are shown in Figures 23 (a) and (b), respectively. The figures indicate, for both Si- and C-faces, basically similar oxide thickness dependences of the growth rate are seen at the partial pressures lower than 0.1 atm to those at above 0.1 atm shown in Section 4, even at the partial pressures lowered to 0.02 atm. Namely, just after the oxidation starts, the oxide growth rates

http://dx.doi.org/10.5772/61082

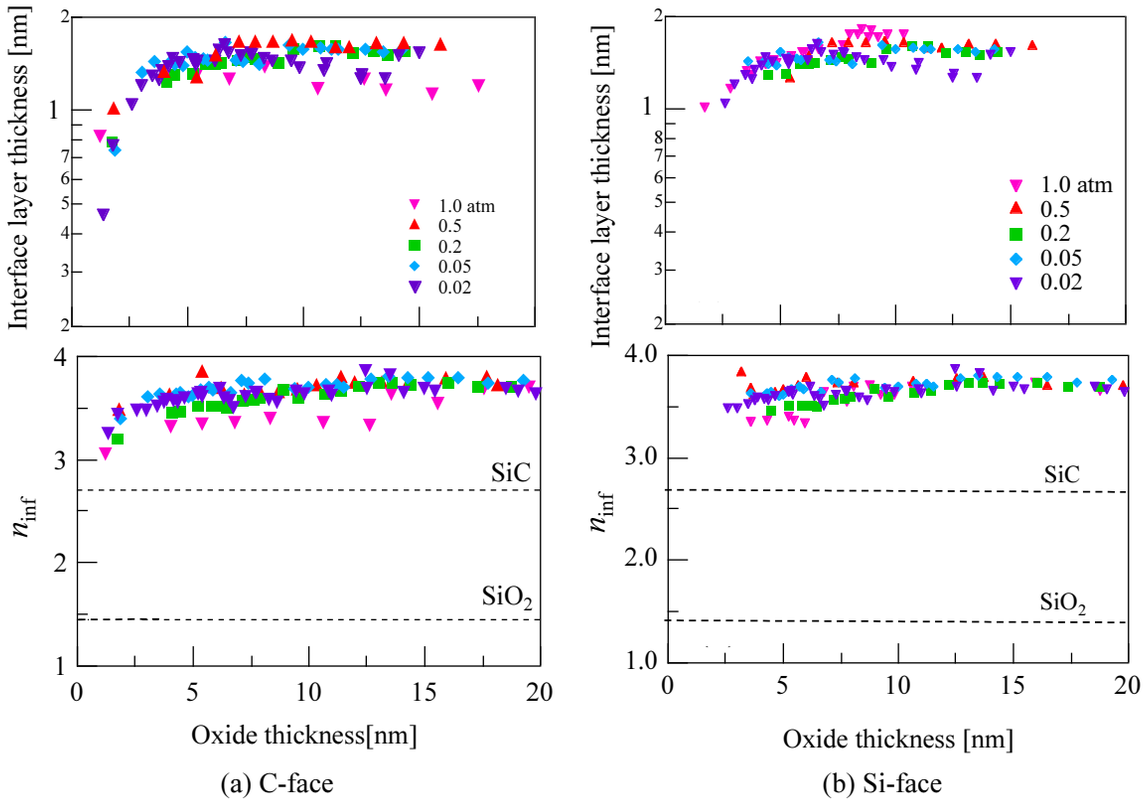

Figure 22. Oxide thickness dependence of interface layer thickness and n_{inf}. at various oxygen partial pressures on (a) the (000-1) C-face and (b) the (0001) Si-face [32].

rapidly decrease and the deceleration rate changes to a gentle one at around 7 nm in oxide thickness (hereafter the two oxidation stages are denoted as the rapid and gentle deceleration stage, respectively).

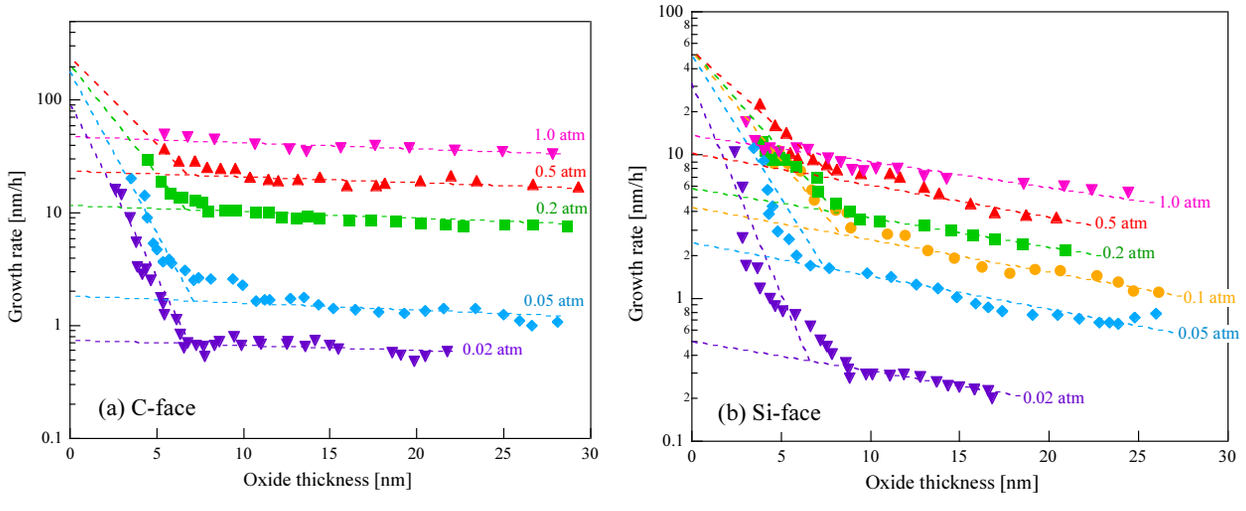

Figure 23. Oxide growth rates as a function of oxide thickness at various oxygen partial pressures on (a) the (000-1) C-face and (b) the (0001) Si-face. Broken lines are fitted to the experimental data using exponential functions [32].

We fitted the experimental data at each partial pressure with two straight lines, as shown by the dotted lines in Figures 23 (a) and (b), and derived the initial growth rate of the two deceleration stages, R_0 and R_1, by extrapolating the straight line to oxide thickness $X = 0$ in the rapid and gentle deceleration stages, respectively. The figures show that the thickness at which the deceleration rate changes from a rapid to a gentle one (termed "deceleration-rate-change thickness X_c "), i.e., the cross point of the two decay lines, is almost constant around 7 nm regardless of the oxygen partial pressure or surface polarity.

Figure 24 shows the oxygen partial pressure dependence of R_0 and R_1 on the C- and Si-faces. Since oxide growth in the thin region was too fast to follow spectroscopic ellipsometry measurements in the case of 1 atm pressure on the C-face, it was hard to estimate the oxide growth rates in the rapid deceleration stage accurately. Thus, the value of R_0 for the C-face at 1 atm is not shown in this figure. The dashed line in Figure 24 shows the data proportional to the oxygen partial pressure and fitted to the R_1 data for the C-face. For both polar faces, the data points of R_1 are almost on the line, suggesting that R_1 is proportional to the partial pressure, though, for the Si-face, R_1 becomes slightly smaller as seen from the linear relation approaching 1 atm. It should be noted that the rates are almost equal for the C- and Si-faces at low pressures, which is different from the fact that the oxide growth rates for the C-face are about 10 times larger than those for the Si-face in the several 10 nm thickness region at atmospheric oxygen pressure [15,18,19,31].

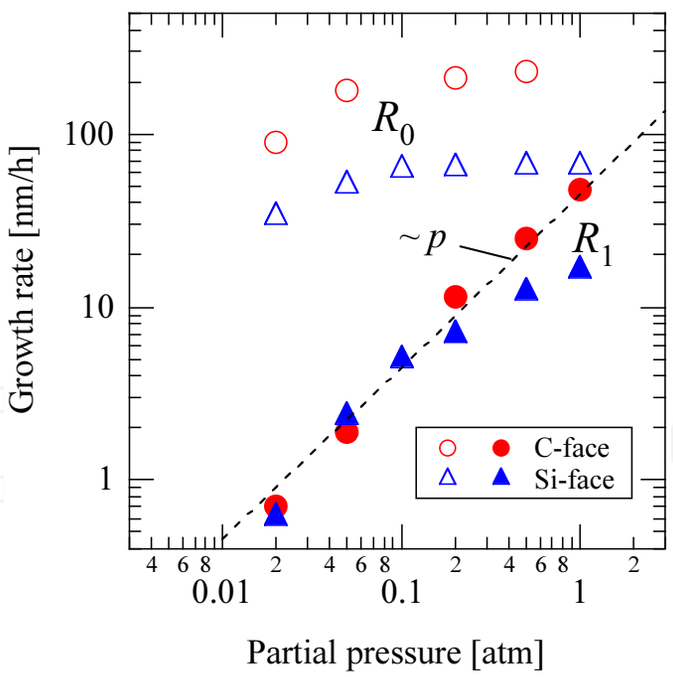

Figure 24. Oxygen partial pressure dependence of the initial growth rate, R_0 (unfilled symbols), and the gentle deceleration growth rate, R_1 (filled symbols), on the C-face (circles) and Si-face (triangles) [32].

We will discuss these results based on the oxidation mechanisms, especially, by use of interfacial Si-C atoms emission model, as follows. Here, we briefly state the essence of the Si

and C emission model that we proposed for a description of the SiC oxidation process [33]. During oxidation, Si and C interstitials are emitted from the SiC/oxide interface, and a decrease in the interfacial reaction rate, k, as expressed by the following function, occurs as the interstitials accumulate inside the oxide near the interface accompanying progress in oxidation,

$$k = k_0 \left(1 - \frac{C_{Si}^{int}}{C_{Si}^{lim}}\right)\left(1 - \frac{C_C^{int}}{C_C^{lim}}\right), \tag{6}$$

where C^{int} and C^{lim} are the concentrations at the interface and the solubility limit in the oxide, respectively, of the corresponding interstitial atoms, i.e., Si and C, and k_0 is the initial interfacial oxidation rate. If the oxide grows only at the interface, the oxide growth rate dX/dt is represented by the equation,

$$N_0 \frac{dX}{dt} = kC_O^{int} \tag{7}$$

where N_0 is the molecular density of SiO_2, and $C^{int}{}_O$ is the concentration of oxygen at the interface. As seen from this equation, a decrease in k corresponds to a decrease in dX/dt. It should be noted that the D-G model corresponds to the case that k is constant regardless of the oxide thickness in this oxidation model.

i. Formation and structures of the interface layers

We have reported [27,28] that the photon energy dependence of the optical constants n_{it} and k_{it} derived from the complex dielectric constants between 2 and 6 eV, covering the direct interband transition energy E_0 of 4H -SiC of 5.65 eV, is similar to that of bulk 4H -SiC, though the absolute values of n_{it} are about 1 larger than those of SiC, which were again confirmed in this study. The similarity in the energy dispersion of the optical constants of the interface layers suggests that the interface layer is not a transition layer between SiC and SiO_2. Rather, it is a layer having a modified structure and/or composition compared to SiC, such as a stressed or interstitials-incorporated SiC layer, locating not on the SiO_2 side but on the SiC side of the SiC/oxide interface.

The experimental results also indicated that the thickness at which the interface layer thickness and the value of n_{inf} becomes constant (i.e., 7 nm) is determined not from the surface polarity or oxygen partial pressure but from the oxide thickness. The Si-C emission model describes this behavior by considering that Si and C atoms are emitted into both directions of the SiC/oxide interface accompanying oxidation at the interface, i.e., into not only the oxide layer but also the SiC layer, and accumulation of interstitial Si and/or C atoms emitted into the SiC substrate may form a layer having similar optical properties as SiC but larger refractive indices compared to SiC. Since accumulation of interstitials is linked to the growth of the oxide, it is considered that growth of the interface layer is saturated at some intrinsic oxide thickness even

if the oxygen pressure is changed. We will discuss the behavior of the interface layer as well as that of X_c, later.

ii. Oxide thickness dependence of oxide growth rate

As mentioned above, there are two oxidation stages in the oxide growth rate curves, i.e., first rapid deceleration and second gentle deceleration. Since the growth rates at each deceleration stage are seen as a straight line in a semi-logarithm plot (shown by broken lines in Figures 23 (a) and (b)) in the respective stage, the oxide thickness dependence of the oxide growth rate can be approximated by the sum of two exponential functions [59] as

$$\frac{dX}{dt} = R_0 \exp\left(-\frac{X}{L_1}\right) - R_1 \exp\left(-\frac{X}{L_2}\right) \tag{8}$$

where R_0 and R_1 ($R_0 >> R_1$) have the same meaning as in Figure 23, i.e., pre-exponential constants, and L_0 and L_1 ($L_0 < L_1$) are the characteristic lengths for the deceleration of oxide growth rate in each oxidation stage, respectively. Equation (8) means that in the thin oxide regime, oxide growth occurs by two ways and they proceed not in series but in parallel because the growth rate is given by the sum of two terms and is chiefly determined by the faster one in each stage. Obviously, the L_0 and L_1 values correspond to the gradients of the fitted line in the rapid and gentle deceleration stage, respectively. As shown in Figure 23, the L_0 value decreases with decreasing partial pressure, which corresponds to the more remarkable rapid deceleration. In contrast, the L_1 value is almost constant regardless of the partial pressure. This suggests that the oxidation process is different between the rapid and gentle deceleration stages. We will discuss these two deceleration stages relevant to the oxide growth mechanism.

iii. Discussion of the two decelerating stages in terms of SiC and Si oxidation mechanisms

The existence of a rapid deceleration stage in the oxide growth rate just after oxidation starts (X < 10 nm) has also been observed for Si oxidation [4,60]. However, in investigations on Si oxidation mechanisms, the cause of the rapid deceleration has not yet been clarified. That is, the Deal-Grove model cannot fully account for the initial rapid deceleration [1]. An empirical equation, i.e., the D-G term plus an exponential term, proposed by Massoud et al.[4], can only reproduce the observed growth rates numerically, but does not provide a physical meaning. The interfacial Si emission model [52] is now believed to be the model that can reproduce the observed oxide growth rate quantitatively very well for Si oxidation. However, the model also cannot reproduce the remarkable rapid deceleration at subatmospheric oxygen pressures, as pointed out by Farjas and Roura [60]. For SiC oxidation, we have tried to reproduce the observed data using Massoud's empirical equation [30,31,50]. Here, we discuss the reasons why two deceleration stages exist in the thickness dependence of oxide growth rate, based on the interfacial Si-C emission model.

The interfacial reaction rate (k in Eq. (6)) is unlikely to depend on the oxygen partial pressure, p, because it corresponds to the rate at which one SiC molecule is changed to one SiO_2 molecule, which should not depend on p. In the thin oxide regime discussed here, the interface oxygen

concentration C^{int}_O can be expressed as $C^{int}_O \sim pC^{lim}o$ by Henry's law, where C^{lim}_O is the solubility limit of oxygen in SiO_2. Therefore, the growth rate in the thin oxide regime, R, should be proportional to p, which is in good agreement with the experimental results in the gentle deceleration stage, i.e., R_1.

According to the Si-C emission model [33], as the number of accumulated atoms increases with oxidation, and is thus proportional to the quantity of oxidized molecules, i.e., the thickness of the oxide X, the variation in k may be approximately given as an exponential function of X in the form of $C\exp(-X/L)$, where C and L are the pre-exponential term and characteristic length, respectively, related to the accumulation of Si and C interstitials at the interface. From these considerations, as well as the fact that R_1 is proportional to p, the gentle deceleration of the oxide growth rate can be attributed to the accumulation of Si and C interstitials near the interface, and given approximately as $dX/dt \sim R_1\exp(-X/L_1)$, which is coincident with the second term in Eq. (8).

If the initial growth rate R_0 in the rapid deceleration stage is also followed by Eq. (7), it can be expressed as $R_0 \sim k_0C^{int}_O/N_0$, where k_0 is the interfacial reaction rate when the oxidation starts. As the value of k_0 is also unlikely to depend on the oxygen partial pressure, R_0 should be proportional to the oxygen pressure. As seen in Figure 24, while R_0 is not proportional to p, it decreases with decreasing p in the low p region. This suggests that R_0, i.e., the rapid deceleration, is not related to the interfacial oxide growth. In the case of Si oxidation, the experimental data show almost no dependence of R_0 with respect to p [4].

We next consider the reason why R_0 is not proportional to but rather is almost independent of the oxygen partial pressure, both for Si and SiC oxidations. It has been considered that oxide growth occurs only or mainly at the Si/oxide (SiC/oxide) interface. However, according to the Si emission model [52] for Si oxidation and the Si and C emission model [33] for SiC oxidation, Si atoms (Si and C atoms) are emitted into the oxide layer, some of which encounter the oxidant inside the oxide to form SiO_2. If the oxide is so thin that, some of the Si atoms emitted can go through the oxide layer and reach the oxide surface, those Si atoms are instantly oxidized to form a SiO_2 layer at the surface. This indicates there exist another oxide growth process other than the oxide formation at the SiC/oxide interface and that due to the oxidation of Si interstitials inside the oxide layers, i.e., the oxide formation by way of the oxidation of Si interstitials at the oxide surface. It is noted that this oxide formation process on the surface has not been considered in the Si emission model for Si oxidation [52]. The oxide growth rate of SiC is, therefore, totally given by the sum of these three oxide formation processes. In the case of oxidation inside the oxide, the probability of the emitted Si interstitials meeting the oxidant inside the oxide should be proportional to the oxygen concentration in the oxide. Therefore, this oxidation process should be proportional to p like R_1, and thus can be excluded as a candidate of the origin of R_0.

In contrast, in the case of oxidation on the oxide surface, the amount of oxygen is thought to be sufficient to oxidize all the Si atoms emitted and appearing on the surface, because the number of oxygen molecules impinging onto the surface from the gaseous atmosphere is several orders larger than the number of emitted Si atoms transmitted through the oxide even if the oxygen pressure is as low as 0.02 atm. Therefore, the oxide growth rate for oxidation on

the oxide surface should be independent of the oxygen partial pressure, which is in good agreement with the behavior of R_0. Besides, the possibility that Si interstitials go through the oxide and reach the oxide surface is considered to decrease rapidly with increasing oxide thickness, and can be given the form $\exp(-X/L_0)$, where L_0 ($<L_1$) is the escape depth of Si atoms from the oxide layer. From these considerations, the rapid deceleration stage of oxide growth rate observed just after oxidation starts is thought to be due to oxidation of Si interstitials on the oxide surface. Therefore, the value of X_c obtained from the experiments of 7 nm indicates that the escape depth of Si atoms from the oxide is estimated to be several nanometers at 1100°C. Since the behavior of Si interstitials other than at the interface should be the same for the C- and Si-faces, it is reasonable that the value of X_c does not depend on the polarity of the SiC faces. Moreover, the fact that the growth rates in the thin regime at low pressures are not very different for the C- and Si-faces can be explained by considering that surface oxide growth is dominant over oxide growth in this stage and oxidation on the oxide surface may proceed independent of the surface polarity.

Theoretical calculations of the growth rates reported so far have not taken into account the surface oxide growth for both Si and SiC oxidations. However, in the extremely thin oxide thickness range and especially at low oxygen partial pressures, the contribution from surface oxide growth as well as those from the interface and internal oxide growth should be taken into account. However, to confirm the argument derived from the experimental results in this study, it is necessary to perform numerical calculations of the oxide growth rates within the framework of the Si-C emission model, taking into account the contribution from oxidation on the surface. In the case of Si oxidation, the interfacial Si emission model [52] cannot reproduce the growth rate in the thin oxide region at sub-atmospheric pressures, as pointed out by Farjas and Roura [60], where the introduction of the contribution from the surface oxide growth may dissolve the disagreement between the calculated and the observed oxide growth rates.

As mentioned above, the X_c value is almost constant around 7 nm regardless of the oxygen partial pressure, though the rapid deceleration stage can be observed more remarkably at lower partial pressures. In the case of Si oxidation, a rapid deceleration stage has also been observed just after oxidation starts, and the thickness corresponding to X_c is also almost independent of the oxygen partial pressure, though the growth rates at X_c depend on the oxygen partial pressure [4,60]. Therefore, it can be stated that X_c is determined only by the thickness of the oxide layer for both the Si and the SiC oxidation cases. It is to be noted that the value of X_c is very close to the thickness at which the interface structures become constant as revealed above. In addition, the pressure dependence of the oxide thickness when the interface layer becomes unchanged also exhibits the same behavior, i.e., they are almost independent of pressure. These results suggest that an interface layer gradually grows during the surface oxide growth and, after transforming to the interfacial and internal oxide growth, the interface layer stops growing. It is considered that the interface layer located on the SiC side of the interface may be oxidized to form SiO_2 and a new interface layer may form on the SiC side, which results in movement of the position of the interface layer in the direction of the SiC substrate with progress in oxidation. Therefore, the brake for the interface layer growth

is considered to be responsible for the abrupt change in growth rate at X_c. Otherwise, during the surface oxide growth, fewer interstitials emit into the SiC-side because the concentration of interstitials in the oxide is quite low; in turn, the emission into the SiC-side increases with accumulation of interstitials in the oxide and then the accumulation of interstitials is saturated when it balances with the progress in oxidation front.

6. Summary

We have employed spectroscopic ellipsometry, one of the methods of observing buried interfaces keeping intact for observing SiC/oxide interfaces to investigate their structures. We have developed the characterization method of the oxide layers and SiC/oxide interfaces, i.e., by using sloped oxide layers, and made clear the depth profile of the refractive indices and interface structures, i.e., there exist interface layers, having high refractive indices compared with those of SiC and SiO_2, the values of which depend on the oxide layer formation method, around 1 nm in thickness, at oxide/SiC interface and only the thickness of the SiO_2 layers changes with oxidation time or oxide thickness. It can be said that the optical properties estimated from the analysis using the single layer model, i.e., the oxide films are assumed to be optically uniform single layer on SiC, are "apparent" features, and it is not true that the optical constants of the oxide layers change with oxidation time or oxide thickness. The results that the refractive indices of the interface are larger than those of both SiC and SiO_2 reveal that the interfaces are neither the transition layers having the composition between SiO_2 and SiC nor those due to interface roughness.

Optical and electrical evaluations of SiC/oxide interface based on the spectroscopic ellipsometry in the visible to deep UV region and the *C-V* measurements by using the same samples for both measurements have been carried out for the samples with both surface polarities, and formed by various oxidation methods and temperatures, including the samples after various POA. Quite good correlations between the changes in refractive indices of the interface layers n_{it} by the oxidation condition and those in interface state density D_{it} are found for all the cases of oxidation conditions. These correlations suggest that the formation of the interface layers with large refractive indices is related to the generation of interface states. It is also found that the wavelength dependences of extinction coefficient of the interface layers k_{it} are quite similar to those of SiC in the entire wavelength range measured, suggesting the presence of layers with a little different band structures from that of bulk SiC, e.g., strained SiC layers. By using the method of inducing interface state density by γ-ray irradiation, we have confirmed that the values of refractive indices of interfaces obtained from spectroscopic ellipsometery are well correlated with the electrical properties of interface, like interface state density, which strongly supports that the values of refractive indices of interface layers are reflected from the electrical properties of interfaces.

We have also developed the observation system in order to perform real-time *in-situ* observation of SiC oxidation for the first time. By using this system, we have observed the occurrence of the oxide growth rate enhancement in the thin oxide regime for the oxidation of SiC both

for Si- and C-faces. We have also observed that the growth rate of SiC for both polar faces can be well represented by the Massoud's empirical equation using the four adjusting parameters. From the differences in temperature and oxygen partial pressure dependences of these parameters, we have discussed on the difference of the oxidation mechanisms between Si-face and C-face of SiC.

Finally, we have studied the oxygen partial pressure dependence of the SiC oxidation process in the initial oxidation stage in details at oxygen partial pressures ranging from 0.02 to 1.0 atm. It was found that regardless of the surface polarity as well as the oxygen partial pressure, an interface layer having modified SiC structures is formed accompanied by oxidation just below the SiC/oxide interface in the same manner, i.e., the thickness and refractive indices of the interface layer increase with an increase in the oxide thickness, the interface layer thickness reaches about 1.5 nm at an oxide thickness of around 7 nm, and then the thickness and structure of the interface layer do not change anymore with further increase in oxide thickness. The oxide thickness dependence of the growth rate at sub-atmospheric oxygen partial pressures down to 0.02 atm is similar to those at 1 atm. Namely, just after the oxidation starts, the oxide growth rate rapidly decreases and the deceleration-rate changes to a gentle mode at around 7 nm in oxide thickness, which is almost the same thickness at which the thickness and the structure of the interface layers become constant. We have shown that the interfacial Si-C emission model can explain the cause for the change in deceleration rate of the oxide growth rate from the oxygen partial pressure dependence and found that the oxide growth due to oxidation of Si interstitials on the oxide surface plays a dominant role in the extremely thin thickness region, less than several nanometers.

Through the studies on SiC/oxide interfaces based on the spectroscopic ellipsometry measurements, we have found the existence of strong correlation between the optical properties of interface, like n_{it}, and the electrical properties, like D_{it}. However, in general, the mechanisms of the relation between the MOS characteristics of SiC, i.e., low carrier mobility and threshold voltage instability, and the interface structures have not been made clear. It is eager to understand the mechanisms of SiC-MOS characteristics in relation to the interface structures. The results obtained suggest the interface structures, i.e., the formation of interface layers with high refractive indices depend on oxide thickness as well as the oxidation conditions. Therefore, it can be said that the process of forming no interface layers or the interface layers with very thin or having lower refractive indices is desirable, by the methods of, for example, using very thin oxide layers. The formation of insulated layers for MOS structures not by oxidation of SiC, but by the deposition of insulator materials, for examples, Si oxide and Al oxide, may be other candidates, though caution should be taken to avoid the proceed of oxidation during the device process performed after the formation of MOS interface. Anyway, the important point is to develop the process based on the information of "true" interface structures obtained by use of non-distractive measurement methods, like ellipsometry, with selecting an appropriate model for the analyses of measured data.

Author details

Sadafumi Yoshida[1*], Yasuto Hijikata[2] and Hiroyuki Yaguchi[2]

*Address all correspondence to: s.yoshida@aist.go.jp

1 Advanced Power Electronics Research Center, National Institute of Advanced Industrial Science and Technology (AIST), Tsukuba, Japan

2 Graduate School of Science and Engineering, Saitama University, Saitama, Japan

References

[1] Deal BE, Grove AG. General relationship for the thermal oxidation of silicon. J Appl Phys 1965;36(12):3770-8.

[2] Taft E, Cordes L. Optical evidence for silicon-carbide oxide interface. J Electrochem Soc 1979;126:131-4.

[3] Aspnes DE, Theeten JB. Optical properties of the interface between Si and its thermally grown oxide. Phys Rev Lett 1971;43(14):1046-9. Dielectric function of Si-SiO_2 and Si-Si_3N_4 mixture. J Appl Phys 1979;50(7):4928. Spectroscopic analysis of the interface between Si and its thermally grown oxide. J Electrochem Soc 1980;127(6): 1359-65.

[4] Massoud HZ, Plummer JD, Irene EA. Thermal oxidation of silicon in dry oxygen growth-rate enhancement in the thin regime. I. Experimental results. J Electrochem Soc 1985;132(11):2685-93. II. Physical mechanisms. *ibid*. 2693-700. Analytical relationship for the oxidation of silicon in dry oxygen in the thin-film regime. J Appl Phys 1987;62(8):3416-23.

[5] Nguyen N, Chandier-Horowitz D, Amirtharaj PM, Pollengrino JP. Spectroscopic ellipsometry determination of the properties of the thin underlying strained Si layer and the roughness at SiO_2/Si interface. Appl Phys Lett 1994;64(20):2688-90.

[6] Suwa T, Teramoto A,.Kumagai K, Abe K, Lie X, Nakao Y, Yamamoto M, Nohira H, Muro T, Kinoshita T, Sugawa S, Ohmi Hattori M. Chemical structure of interfacial transition layer formed on Si (100) and its dependence on oxidation temperature, annealing in forming gas, and difference in oxidizing species. Jpn J Appl Phys 2013;52:031302.

[7] Hebert KJ, Zafar S, Irene EA, Kuehn R, McCarthy TE, Demirliogle EK. Measurement of the refractive index of thin SiO_2 films using tunneling current oscillation and ellipsometry. Appl Phys Lett 1996;68(2):266-8.

[8] Herzinger CM, Johs B, McGahan WA, Woollan A. Ellipsometric determination of optical constants for silicon and thermally grown silicon dioxide via a multi-sample, multi-wavelength, multi-angle investigation. J Appl Phys 1998;83(6):3323-36.

[9] Jernigan GG., Stahlbush RE, Das MK, Cooper Jr JA, Lipkin LA. Interfacial differences between SiO_2 grown on 6H-SiC and on Si(100). Appl Phys Lett 1999;74(10):1448-50. Effect of oxidation and reoxidation on the oxide-substrate interface of 4H- and 6H-SiC. *ibid*. 2000;77(10):1437-9.

[10] Zhu X, Lee HD, Feng T, Ahyi AC, Mastrongiovann D, Wan A, Garfunkel E, Williams JRG, Feldman LC. Structure and stoichiometry of (0001) 4H-SiC/oxide interface. Appl Phys Lett 2010;97:071908.

[11] Watanabe H, Hosoi T, Kirino T, Kagei Y, Uenishi Y, Chanthaphan A, Yoshigoe A, Teraoka Y, Shimura T. Synchrotron X-ray photoelectron spectroscopy study on thermally grown SiO_2/4H-SiC (0001) interface and its correlation with electrical properties. Appl Phys Lett 2011;99:021907.

[12] Zheleva T, Lelis A, Duscher G, Liu F, Levin I, Das M. Transition layers at the SiO_2/SiC interface. Appl Phys Lett 2008;93:022108.

[13] Biggerstaff TL, Reynolds Jr CL, Zheleva T, Lelis A, Habersat D, Henry S, Ryu S-H, Agawal A, Dusher G. Relationship between 4H-SiC/SiO_2 transition layer thickness and mobility. Appl Phys Lett 2009;95:032108.

[14] Hatakeyama T, Matsuhata H, Suzuki T, Shinohe T, Okumura H. Microscopic examination of SiO_2/4H-SiC interfaces. Mater Sci Forum 2011;679-680:330-3.

[15] Suzuki A, Ashida H, Furui N, Maneno K, Matsunami H. Thermal oxidation of SiC and electrical properties of Al-SiO_2-SiC MOS structure. Jpn J Appl Phys 1982;21(4): 579-85.

[16] Zheng Z, Tresslerand RE, Spear KE. Oxidation of single-crystal silicon carbide, Part 1 Experimental studies. J Electrochem Soc 1990;137(3):854-8. Part II. Kinetic model. *ibid.* 1990;137(9):2812-6.

[17] Fung CD, Kopanski JJK. Thermal oxidation of 3C-silicon carbide single-crystal layers on silicon. Appl Phys Lett 1984;45(7):757 -9.

[18] Song Y, Dhar S, Feldman LC, Chung G, Williams JR. Modified Deal Grove model for the thermal oxidation of silicon carbide. J Appl Phys 2004;95:4953-7.

[19] Ray EA, Rozen J, Dhar S, Feldman LC, Williams JR. Pressure dependence of SiO_2 growth kinetics and electrical properties on SiC. J Appl Phys 2008;103:023522.

[20] Szilagyi E, Petrik P, Lohner T, Koos AA, Fried M, Battistlig G. Oxidation of SiC investigated by ellipsometry and Rutherford backscattering spectrometry. J Appl Phys 2008;104:014903.

[21] Hazura S, Chakraborty S, Lai PT. Density profiles and electrical properties of thermally grown oxide nanofilms on p-type 6H-SiC (00001). Appl Phys Lett 2004;85(23): 5580-2.

[22] Correa SA, Radtke C, Soares G.V, Miotti L, Baumiol IJR, Dimitriyev S, Ham J, Hold L, Kong F, Stedile FC. Effects of nitrogen incorporation on the interface layer between thermally grown dielectric films and SiC. Appl Phys Lett 2009;94:251909.

[23] Tsuchida H, Kamata I, Izumi K. Infrared analysis of SiO_2 films on the 6H-SiC surfaces. Appl Surf Sci 1997;117/118:225-9.

[24] Yoshikawa M, Seki H, Inoue K, Nanen Y, Kimoto T. Characterization of inhomogeneity in silicon dioxide films on 4H-silicon carbide epitaxial substrate using a combination of Fourier transform infrared and cathodoluminescence spectroscopy. Appl Spectroscopy 2014;68(10):1176-80.

[25] Iida T, Tomioka Y, Hijikata Y, Yaguchi H, Yoshikawa M, Ishida Y, Okumura H, Yoshida S. Characterization of oxide films on SiC by spectroscopic ellipsometry. Jpn J Appl Phys 2000;39(10B):L1054-6.

[26] Iida T, Tomioka Y, Yoshimoto K, Midorikawa M, Tsukada H, Orihara M, Hijikata H, Yaguchi H, Yoshikawa M, Itoh H, Ishida Y, Yoshida S. Measurements of the depth profile of the refractive indices in oxide films on SiC by spectroscopic ellipsometry. Jpn J Appl Phys 2002;41(2A):800-4.

[27] Hashimoto H, Hijikata Y, Yaguchi H, Yoshida S. Optical and electrical characterizations of 4H-SiC-oxide interfaces by spectroscopic ellipsometry and capacitance-voltage measurements. Appl Surf Sci 2009;255:8648-53.

[28] Seki H, Wakabayashi T, Hijikata Y, Yaguchi Y, Yoshida S. Characterization of 4H-SiC-SiO_2 interfaces by deep ultraviolet spectroscopic ellipsometer. Mater Sci Forum 2009;615-617:505-8.

[29] Kakubari K, Kuboki R, Hijikata Y, Yaguchi H, Yoshida S. Real time observation of SiC oxidation using an *in-situ* ellipsometer. Mater Sci Forum 2006;527-529:1031-4.

[30] Yamamoto T, Hijikata Y, Yaguchi H, Yoshida S. Growth rate enhancement of (000-1)C-face silicon-carbide oxidation in thin oxide regime. Jpn J Appl Phys 2007;46(32):L770-2.

[31] Yamamoto T, Hijikata Y, Yaguchi H, Yoshida S. Oxide growth rate enhancement of silicon carbide (0001) Si-faces in thin oxide regime. Jpn J Appl Phys 2008;47(19): 7803-6.

[32] Kouda K, Hijikata Y, Yagi S, Yaguchi H, Yoshida S. Oxygen partial pressure dependence of the SiC oxidation process studied by in-situ spectroscopic ellipsomerty. J Appl Phys 2012;112:024502.

[33] Hijikata Y, Yaguchi H, Yoshida S. A kinetic model of silicon carbide oxidation based on the interfacial silicon and carbon emission phenomena. Appl Phys Express 2009;2:021203.

[34] Yoshikawa M, Satoh K, Ohshima T, Itoh H, Nashiyama I, Yoshida S, Okumura H, Takahashi, Ohnishi K. Depth profile of trapped charges in oxide layer of 6H-SiC metal-oxide-semiconductor structures. J Appl Phys 1996;80(1):282-7.

[35] Tomioka Y, Iida T, Midorikawa M, Tukada H, Yoshimoto K, Hijikata Y, Yaguchi H, Yoshikawa M, Ishida Y, Kosugi R, Yoshida S. Characterization of the interfaces between SiC and oxide films by spectroscopic ellipsometry. Mat Sci Forum 2002;389-393:1029-32.

[36] Cho W, Kosugi R, Senzaki J, Fukuda K, Arai K, Suzuki S. Study on electron trapping and interface states of various gate dielectric materials in 4H-SiC metal-oxide-semiconductor capacitors. Appl Phys Lett 2000;77(13):2054-6.

[37] Dunham ST. Interaction of silicon point defects with SiO_2 films. J Appl Phys 1992;71(2):685-96.

[38] Cobet C, Wilmers K, Wethkamp T, Edwards NV, Esser N, Richter W. Optical properties of SiC investigated by spectroscopic ellipsometry. Thin Solid Films 2000;364:111-3.

[39] Zollner S, Chen JG, Duda E, Wetteroth T, Wilson SR, Hilfiker JN. Dielectric functions of bulk 4H and 6H SiC and spectroscopic ellipsometry studies of thin SiC films on Si. Appl Phys Lett 1999;85(12):8353-61.

[40] Lindquist OPA, Jarrendhl K, Peters S, Zettler JT, Cobet C, Esser N, Aspnes DE, Henry A, Edwards NV. Ordinary and extraordinary dielectric function of 4H- and 6H-SiC from 3.5 to 9.0 eV. Appl Phys Lett 2001;78(18):2715-7.

[41] Ishida Y, Takahashi T, Okumura H, Jikimoto T, Tsuchida H, Yoshikawa M, Tomioka Y, Hijikata Y, Yoshida S. The investigation on 4H-SiC/SiO_2 interfaces by optical and electrical measurements. Mater Sci Forum 2002;389-393:1013-6.

[42] Hijikata Y, Yaguchi H, Yoshikawa M, Yoshida S. Composition analysis of SiO_2/SiC interfaces by electron spectroscopic measurements using slope-shaped oxide films. Appl Sur Sci 2001;184:161-6.

[43] Fukuda K, Kato K, Senzaki J, Kojima K, Suzuki T. 4H-SiC MOSFETs on C(000-1) face with inversion channel mobility of 127 cm^2/Vs. Mater Sci Forum 2004;457-460:1417-20.

[44] Allerstam F, Olafsson HO, Gugjonsson G, Dochev D, Sveinjornsson EO, Rodle T, Jos R. A strong reduction in the density of near-interface traps at the SiO_2/4H-SiC interface by sodium enhanced oxidation. J Appl Phys 2007;101:124502.

[45] Chung GY, Williams JR, Tin CC, McDonald K, Farmer D, Chanana RK, Pantelides ST, Holland OW, Feldman LC. Interface state density and channel mobility for 4H-SiC MOSFETs with nitrogen passivation. Appl Surf Sci 2001;184:399-403.

[46] Hijikata Y, Yaguchi H, Yoshida S. Effect of Ar post-oxidation annealing on oxide-4H-SiC interfaces studied by capacitance to voltage measurements and photoemission spectroscopy. J Vac Sci Technol 2005;A23(2):298-303.

[47] Cantin JL, von Bardeleben HH, Shinkin Y, Ke Y, Devaty RP, Choyke WJ. Identification of the carbon dangling bond center at the 4H-SiC/SiO_2 interface by an EPR study in oxidized porous SiC. Phys Rev Lett 2004;92(1):015502.

[48] Midorikawa M, Hijikata Y, Yaguchi H, Yoshikawa M, Kamiya T, Yoshida S. Characterization of SiC/oxide films interfaces by spectroscopic ellipsometer (II), Extended Abstracts, The 49th Spring Meeting, 2009, The Japan Society of Applied Physics and Related Societies. p.433.

[49] Goto D, Hijikata Y, Yagi S, Yaguchi H. Differences in SiC thermal oxidation process between crystalline surface orientations observed by in-situ spectroscopic ellipsometry. J Appl Phys 2015;117:095306.

[50] Yamamoto T, Hijikata Y, Yaguchi H, Yoshida S. Oxygen-partial-pressure dependence of SiC oxidation rate studied by *in-situ* spectroscopic ellipsometry. Mater Sci Forum 2009;600-603:667-70.

[51] Grove AS. Physics and Technology of Semiconductor Devices, John Wiley & Sons, New York, 1967, p.31.

[52] Kageshima H Shiraishi K, Uematsu M. Universal theory of Si oxidation rate and importance of interfacial Si emission. Jpn J Appl Phys 1999;38(9A/B):L971-4.

[53] Ogawa S, Takakuwa Y. Rate-limiting reactions of growth and decomposition kinetics of very thin oxides on Si (001) surfaces studied by reflection high-energy electron diffraction combined with Auger electron spectroscopy. Jpn J Appl Phys 2006;45(9A): 7063-79.

[54] Watanabe T, Tatsumura K, Ohdomari I. New linear-parabolic rate equation for thermal oxidation of silicon. Phys Rev Lett 2006;96:196102.

[55] Ueshima M, Kageshima H, Shiraishi K. Simulation of high-pressure oxidation of silicon based on the interfacial silicon emission model. Jpn J Appl Phys 2000;39(10A):L952-4. Simulation of wet oxidation of silicon based on the interfacial silicon emission model and comparison with dry oxidation. J Appl Phys 2001;89(3): 1948-53.

[56] Hijikata Y, Yaguchi H, Yoshida S, Tanaka Y, Kobayashi K, Nohira H, Hattori T. Characterization of oxide films on 4H-SiC epitaxial (000-1) faces by high-energy-resolution photoemission spectroscopy: comparison between wet and dry oxidation. J Appl Phys 2006;100:053710.

[57] Takahashi K, Nohira H, Hirose K, Hattori T. Accurate determination of SiO_2 film thickness by X-ray photoelectron spectroscopy. Appl Phys Lett 2003;83(16):3422-4.

[58] Takaku T, Hijikata Y, Yaguchi H, Yoshida S. Observation of SiC oxidation in ultra-thin oxide regime by in-situ spectroscopic ellipsometry. Mater Sci Forum 2009;615-617:509-12.

[59] Kouda K, Hijikata Y, Yaguchi H, Yoshida S. *In-situ* spectroscopic ellipsometry study of SiC oxidation at low oxygen-partial-pressures. Mater Sci Forum 2010;645-648:813-6.

[60] Farjas J, Roura P. Oxidation of silicon: further tests for the interfacial silicon emission model. J Appl Phys 2007;102:054902.